

FINAL REPORT

for

Contract No. NAG2-62

Period: September 1, 1980 to August 31, 1983

HIGH ACCURACY HEAT CAPACITY MEASUREMENTS

THROUGH THE LAMBDA TRANSITION OF HELIUM

WITH VERY HIGH TEMPERATURE RESOLUTION

(NASA-CR-177037) HIGH ACCURACY HEAT
CAPACITY MEASUREMENTS THROUGH THE LAMBDA

N86-30555

TRANSITION OF HELIUM WITH VERY HIGH
TEMPERATURE RESOLUTION Final Report, 1 Sep.

Unclas

1980 - 31 Aug. 1983 (Stanford Univ.) 51 p G3/77 43234

William M. Fairbank

William M. Fairbank
Professor of Physics
Principal Investigator

John A. Lipa

John A. Lipa
Senior Research Associate
Project Leader

Stanford University
Stanford, CA 94305

May, 1984

first apparatus was successful in demonstrating capability, a number of technical difficulties were uncovered, and a new thermal control system was constructed. This device proved to be entirely adequate for the desired measurements and a large quantity of high resolution data was obtained. Two main experiments were performed, one with a 3 mm high helium sample and the other with a 0.3 mm high sample. The results from the first experiment were analyzed to give the exponent value $\alpha = -0.0127 \pm .0026$, which can be compared with the theoretical prediction, $\alpha = -.007 \pm .006$. Analysis of the second, higher accuracy experiment was not completed in the contract period. This data is now being analyzed under separate funding. While our results show somewhat improved agreement with theory over than obtained previously, a discrepancy with results obtained at higher pressures now exists. In this regime, exponents in the range $-.022 \leq \alpha \leq -.026$ were found previously. New measurements are planned to study this potential conflict.

In the following section we give a short description of the theoretical background and motivation for the present work, and discuss some of the previous experiments in the area. In section 3 we describe the initial apparatus and results, and in section 4 we describe the more advanced system and the data obtained with it. In the appendices we reproduce the publications that have resulted to date and give a listing of the best heat capacity data currently available.

I. INTRODUCTION

Experimental tests of the Renormalization Group (RG) predictions¹ for cooperative phase transitions generally involve curve fitting to experimental data and extraction of parameters of theoretical interest. The quality of such tests depends on the accuracy and dynamic range of the data and the degree to which the system being studied represents an "ideal" case. For the λ -transition of helium the dynamic range available is the maximum for any known substance, extending from $t = |1-T/T_\lambda| \sim 10^{-3}$ to about 3×10^{-8} depending on the degree to which corrections for the effect of gravity can be accepted. The interaction potential between helium atoms is considered to be well represented by a short range force model due to the extremely rapid decay with distance of the van der Waals interaction. Because of the quantum nature of the order parameter, a two-dimensional vector representation is required, but this difference from most other fluid transitions poses no significant difficulty for the comparison of theory with experiment. From a practical point of view, the lambda transition is the most ideal experimental system since impurity effects are negligible, no special knowledge of the system density is required, and the compressibility is only weakly singular at the transition.

Under NASA-Ames Contract # NAG2-62 we performed a new measurement of the heat capacity singularity of helium at the lambda transition with the aim of improving tests of the RG predictions for the static thermodynamic behavior near the singularity. The goal of the project was to approach as closely as possible to the λ -point while making heat capacity measurements of high accuracy. To do this we made use of a new temperature sensor capable of unprecedented resolution near the λ -point, and two thermal control systems. The first system was modified from a unit initially used for high resolution thermometer testing. With this apparatus we performed preliminary measurements and demonstrated the capability to obtain data of the required resolution. While this

II. THEORETICAL BACKGROUND

The most advanced tests of the RG predictions for cooperative transitions are currently from experiments performed near the lambda transition. As is well known, this system has a number of experimental advantages not found at other transitions. Since the system is superfluid below the transition, thermal relaxation times are short, and even above the transition temperature, the thermal conductivity diverges. Also, since it is a fluid system, the problems with strains and crystal defects encountered with solids are avoided. The transition temperature itself is conveniently accessible and in a region where high resolution thermometry is well developed, and where the advantages of superconductivity can be readily applied. The divergence of the compressibility is very weak, in contrast to the behavior near a critical point, avoiding gravity rounding from this effect; and no special care is needed in setting the sample density. These advantages have facilitated the collection of a wide body of accurate data extending to $t \sim 10^{-6}$ on which tests of the RG predictions can be made. At present the most useful data sets for accurate exponent determination have been obtained by Ahlers and co-workers: these include isobaric thermal expansion coefficient data,² heat capacity measurements at the vapor pressure³ and superfluid density measurements⁴. Also of major importance are the heat capacity measurements of Gasparini and Moldover⁵ as a function of ^3He concentration. Many other experiments have been reported, but generally these have either been analyzed in a restricted way, or are of lower accuracy. These experiments allow us to determine two exponents characterizing leading singularities, α and ζ , describing the divergence of the heat capacity and the superfluid density respectively:

$$C_p = \frac{A}{\alpha} t^{-\alpha} (1 + D t^x + \dots) + B \quad (1)$$

$$\frac{\rho_s}{\rho} = A_\rho t^\zeta (1 + D_\rho t^x + \dots) \quad (2)$$

where ρ and ρ_s are the total and superfluid densities, respectively.

The RG calculations give predictions¹ for the exponents α , ζ , x , the coefficient ratios A/A' , D/D' and D'/D_ρ and the difference $B-B'$, where the primed quantities refer to equation (1) below the transition. In addition, the universality hypothesis predicts that the above quantities will be independent of "irrelevant" variables, in this case the pressure and ³He concentration, and scaling predicts that $\alpha = \alpha'$. In Table 1 we list the predicted values for the above quantities, along with previous experimental results.

The most precise determination of a leading exponent reported to date is from the superfluid density data. This is because equation (2) does not contain a parameter equivalent to B in equation (1) easing the curve fitting task considerably, and also because ρ_s has been determined from very precise second sound velocity measurements. The agreement with theory shown in Table 1 is very good, and recently Ahlers⁶ has reported that even better agreement can be obtained if equation (2) is modified by replacing A_ρ with $A_0 + A_1(\rho)t$. In this case, with x set at 0.5, he obtains $\zeta = 0.6716 \pm .0004$, which is within the range of uncertainty of the theoretical estimate. At face value this appears to be very strong support for the RG predictions, but on closer examination there are some remaining difficulties. These stem from the use of second sound to determine ρ_s . The basic relationship for the conversion is

$$\frac{\rho_s}{\rho_n} = \frac{U_2^2 C_p}{S^2 T} + \dots \quad (3)$$

TABLE I

Comparison of parameter values at the lambda point predicted by the RG method with those obtained experimentally. Quantities in parentheses represent constraints.

Parameter	$\alpha(=\alpha')$	A/A'	x	D/D'	$B-B'$	ζ	D'/D_ρ
RG predictions	$-.008$ $\pm .003$	1.03	0.521 $\pm .006$	1.17	0	$.669$ $\pm .002$	$.15$ $\pm .18$
ρ_s data	—	—	$.5 \pm .1$	—	—	$.6749$ $\pm .0007$	$-.17$
Isobaric expansion data	$-.026$ $\pm .004$	1.112 $\pm .022$	(=.5)	1.29 $\pm .25$	(=0)	—	$\pm .04$
$^3\text{He} - ^4\text{He}$ mixtures	$-.022$	1.088	(=.5)	—	(=0)	—	—

where U_2 is the second sound velocity, $\rho_n = \rho - \rho_s$, and S is the entropy. This equation is based on the two-fluid model of He-II, and is assumed reliable to the order of 0.1%. Independent verification by alternative measurements of ρ_s show reliability to a level of about 1% over a restricted temperature range, but no measurements yet exist to fully support this assumption; nor have dispersion measurements been made near T_λ . More importantly, even if (3) can be shown to be correct to the required accuracy, the determination of ζ from the velocity of second sound inevitably involves a knowledge of the heat capacity singularity via the quantity C_p . The velocity data of Greywall and Ahlers was originally converted to ρ_s data using a logarithmic form for C_p , with $\alpha = 0$. As is now well known, α' is probably slightly negative with a best value given in Table 1 in the range $-.016$ to $-.026$. Since C_p is a multiplicative factor in (3) the exponent for ρ_s is dependent on α , no matter how accurately the exponent of U_2 is determined. We have performed numerical studies of this effect and find that the perturbation of ζ is about one third the uncertainty of α' . Thus a change of α' from zero to $-.026$ would lead to a correction of ζ of 0.008, twenty times the estimated uncertainty in this quantity, and throwing it outside the range of acceptable agreement with theory. Clearly the determination of ζ from second sound velocity data must be subordinated to some extent to the prior determination of α' . This leads us to consider the heat capacity singularity to be the primary source of tests of the RG predictions, at least for the present. The remainder of this section will be devoted to a discussion of this topic.

Unfortunately, in spite of a number of experimental measurements, the value of α is not well determined. The isobaric thermal expansion coefficient data of Mueller et al.² give $\alpha = -.026 \pm .004$, which is probably the most commonly quoted value in the literature. This is notwithstanding excellent

heat capacity measurements by Ahlers³ extending down to $t \sim 10^{-6}$, which will be discussed later. The use of the expansion coefficient data as a function of pressure has the advantage that more data can be included in the fitting, but allowance must be made for the pressure dependence of the coefficients A and D.

The heat capacity singularity has also been studied as a function of ³He concentration by a number of workers^{5,7}. Some of the data has been analyzed by Gasparini and Gaeta⁸ using the function in (1). They conclude that the universality hypothesis is well supported by the data in the range $2 \times 10^{-6} < t < 3 \times 10^{-3}$, and for ³He mole fractions in the range $.01 < x < .39$. The best fit parameters are $\alpha = -.022$ and $A/A' = 1.088$. These values are quite close to those obtained by Mueller et al. along the lambda line.

We mentioned above that the highest resolution data³ at the saturated vapor pressure is not the source of the commonly quoted values for the exponents and other parameters. Gasparini and Gaeta have reexamined this data and the somewhat less accurate data of Gasparini and Moldover⁵. They obtain $\alpha (= \alpha') = -.0163$ and $A/A' = 1.068$. With the constraints $\alpha = \alpha' = -.026$, $A/A' = 1.11$, and $D/D' = 1.11$, (essentially the best fit values of Mueller et al.), marked systematic deviations were observed. Also the deviations are similar for the two completely independent experiments. The more recent measurements of Takada and Watanabe⁷ also indicate that α might be of the order -0.016 to -0.018 on the vapor pressure line. These difficulties indicate that further clarification is needed both to determine the exponent value at the lambda line and to evaluate the extent to which universality is supported. This need is all the more urgent in view of the central role that the lambda transition plays in the testing of the basic theory of cooperative transitions. It is most unfortunate that the highest resolution heat capacity measurements at the vapor pressure are

not well reconciled with the other measurements. Not only do they weaken the support for universality and the RG predictions in general, but they also impede the use of second sound to give the superfluid density exponent as described above.

Lambda Transition Broadening

Considering first the effect of gravity alone, the heat capacity of a sample of helium of height h reaches a finite maximum at a reduced temperature interval t_m below the lambda point given by

$$t_m = \frac{\rho g h}{T_\lambda} \left(\frac{dP}{dT} \right)_\lambda^{-1} \quad (4)$$

where ρ is the density of the fluid, and $(dP/dT)_\lambda$ is the slope of the lambda line. Between the lambda "point" and the temperature given by (4) the helium is in a two-phase region with co-existing helium-I and helium-II, and the heat capacity curve is highly distorted. Outside this region we can expand the deviation from the ideal heat capacity, C_0 , in the form

$$\Delta C_g = C_g - C_0 = \frac{A}{2} \frac{t_m}{t} + \frac{A}{6} \left(\frac{t_m}{t} \right)^2 + \dots \quad (5)$$

where C_g is the heat capacity in a gravity field and A is the coefficient of the assumed logarithmic singularity in C_0 . A similar formula can be developed for small but non-zero α . It can be seen from equations (4) and (5) that the perturbation due to gravity is in first order directly proportional to the height of the sample, dictating that this quantity be minimized in any high resolution experiment.

On the other hand, the divergence of the superfluid healing length below the transition dictates a large sample for an accurate representation of C_0 . An exact calculation of this effect is not yet available, but an approximate idea of the magnitude can be obtained by the argument below.

Near the transition, the healing length, r , diverges as

$$r = r_0 t^{-2/3}$$

where $r_0 \approx 2 \times 10^{-8}$ cm. For a horizontal disc-shaped sample, a fraction of the volume $2r/h$ is within one healing length of the boundaries. If the relative distortion of the specific heat in this surface layer is x (<1), then the relative error in the measurement of the total specific heat is

$$\frac{\Delta C}{C_0} \approx \frac{2rx}{h}$$

Thus if we assume $x = 20\%$, and we require that the distortion of the measurement be no more than 1% say, then we must have

$$h > 4 \times 10^{-7} t^{-2/3} \text{ cm}$$

The competition between the effect and the gravity effect above leads to an optimum sample height h which minimizes the combined distortion and maximizes the resolution that can be attained.

A straightforward minimization of the combined effect leads to an optimum height of 1.3 mm and a maximum resolution $t \sim 2 \times 10^{-8}$ assuming a 1% distortion. However, we can clearly do better than this because equation (3) can be used to correct for the gravity effect. At some point it will probably also be possible to correct for the finite size effect in the region where it is small, but here we will ignore this. A slightly more complex calculation indicates that the limit set by the uncertainty in the gravity effect is near $h \approx 0.48$ mm and $t \sim 2.8 \times 10^{-9}$. While of course it is an exciting prospect to contemplate measurements at this resolution, it must be pointed out that a number of difficulties exist. First, the lambda point is not clearly marked in heat capacity measurements; instead the most prominent feature is the maximum, C_m , located an interval t_m below the point of interest. As the resolution is increased beyond t_m the extrapolation to T_λ becomes less certain. Second, the shape

of the heat capacity curve in the neighborhood of C_m will be distorted somewhat by the finite size effects at the He-I/He-II interface; and third, in the region of long correlation length there may be an appreciable gravitational correction due to the pressure gradient which is explicit in the free energy, in addition to the implicit contribution we have calculated above. In spite of these potential problems, it appears that there are reasonable grounds for expecting to obtain a useful resolution of $t = 10^{-8}$ or better.

III. INITIAL EXPERIMENTS

In the period from 1977 to 1980 we developed a new high resolution thermometer (HRT) capable of resolving to approximately 6×10^{-10} deg at the λ -point in a 1 Hz bandwidth. Since this thermometer had essentially zero dissipation in comparison with other lower resolution devices, we were in an excellent position to explore the heat capacity singularity with much higher resolution than previous investigators. To do this, three steps were necessary: a suitable sample had to be constructed, the thermal enclosure had to be modified, and a method of measurement had to be selected. Each of these steps are described below, followed by a description of the results obtained with two different calorimeters.

Calorimeters: Previously, two types of calorimeters have been used: those with some form of valve, and totally sealed high pressure containers. We chose to use a calorimeter incorporating a low temperature valve for a number of reasons: The need for a massive structure to withstand the high internal pressures at room temperature was avoided, as was the need for a helium temperature filling system; calorimeter replacement was relatively simple since it was empty at room temperature; and the sample depth could be adjusted during a run to explore the extent of rounding effects. On the other hand, the addition of the valve actuator to the control system described below turned out to be a significant development task due to the large heat leak from the room temperature end. Figure 1 shows a cross-section of the basic calorimeter design. The helium space is a flat annular chamber approximately 2.5 cm in diameter and up to 3 mm in height. The height was varied by changing the lower section of the calorimeter. The valve assembly consisted of a screw-threaded plunger in the top section together with a copper diaphragm approximately 0.4 mm thick. The diaphragm was coated with indium on the inside surface, which could be pressed against a circular copper knife edge

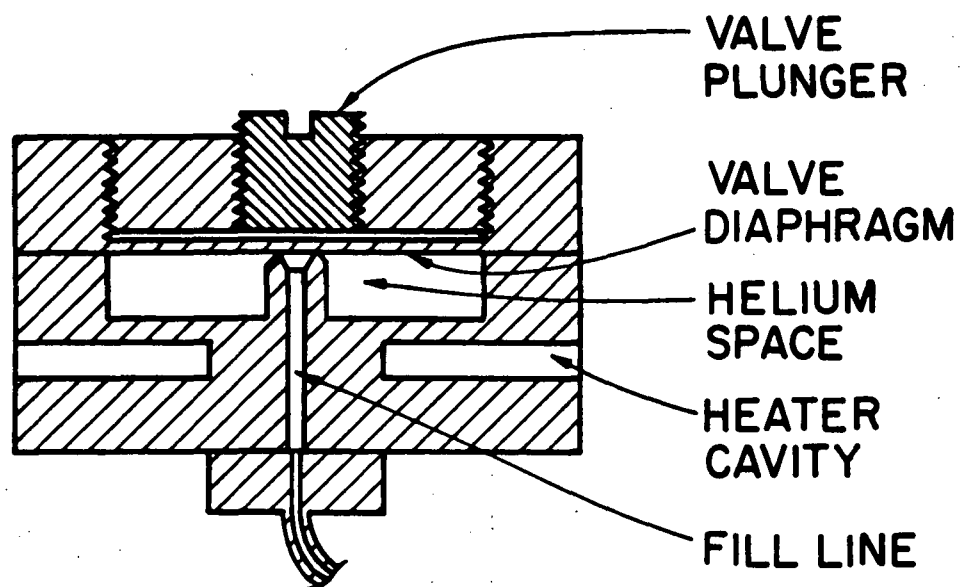


Figure 1: Cross-section of calorimeter

located in the center of the lower section. A capillary filling tube was located at the center of the knife-edge circle. Heaters and thermometers were attached to the lower section of the calorimeter. Initially a brass calorimeter was used since it was more easily constructed and appeared to have an adequately short thermal response time. Some distortion in the heat capacity measurements was observed that appeared to be due to temperature gradients in the calorimeter, so later work used OFHC copper as the construction material.

Thermal Control System: The 4" diameter thermometer test system was upgraded to include a second isolation stage and a calorimeter mounting plate located on top of the HRT. A schematic view of the system is shown in Figure 2. The temperatures of the second isolation stage and the 2° K stage were controlled by carbon thermometers and heaters in integrating servo loops. All feedthroughs to the calorimeter and the HRT were thermally anchored at each stage. As mentioned above, a valve handle actuator was also added. This device consisted of two concentric tubes, one of which was used to turn the valve plunger on the calorimeter by means of a screwdriver actuator, while the other tube supplied a counter-torque to the calorimeter body to reduce the stress on the low heat-leak support structure. The other main features of the thermal control system were the magnet for generating the flux for the HRT, the continuously pumped "cold finger" for maintaining an operating temperature below the λ -point, and the SQUID magnetometer assembly used as the readout system for the HRT.

Method of Measurement of Heat Capacity: Since we were more interested in the curvature of the heat capacity function with temperature than in the absolute values, we decided to use a continuous heating method of measuring C_s . In this method constant power was supplied to the calorimeter and the resulting change of temperature with time was measured. This method was first used

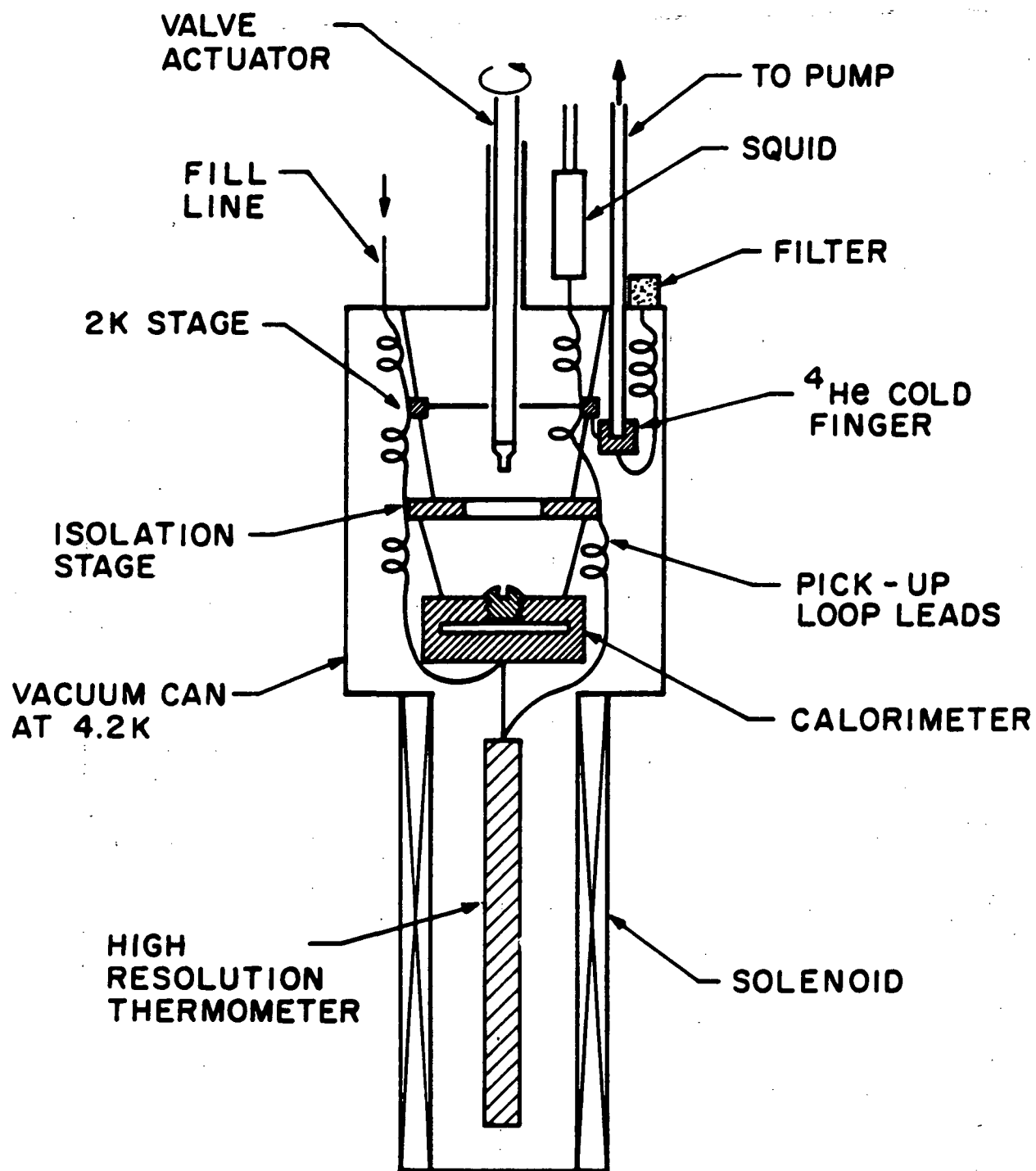


Figure 2: Schematic view of small thermal control system

by Buckingham and Fairbank in their pioneering measurements near the λ -point. By keeping the temperature of the thermal control system slightly below that of the calorimeter, data could also be taken while cooling, giving a useful check on the degree of equilibrium within the sample. Further checks were made by collecting data at different heating rates over the range 10^{-8} to 10^{-9} deg/sec, and by varying the temperature offset between the thermal control system and the calorimeter. Due to the uncertainties in the sample mass and the temperature scale, only rough absolute values of heat capacity were obtained in the early measurements with the small system. Nevertheless, reasonable agreement was found with previous experiments in the regions of overlap.

The constant power method of measuring heat capacity has the advantages that a large amount of information is collected quickly, and the degree of non-equilibrium can be easily assessed by varying the heating rate, but it is particularly sensitive to variations in the heat leak to the sample during the period of the measurements. In the present experiment, there were two main sources of such variations: random fluctuations in the temperature of the inner stage of the thermal control system, and effects due to residual helium in the calorimeter fill line. The first effect set a lower limit on the heating and cooling rates at which useful data could be obtained. This limit was about 10^{-9} deg/sec, somewhat dependent on the details of a particular run. The second effect can be eliminated by evacuation of the fill line, and its absence can be predicted by monitoring the pressure in this line. Experimentally, it was determined that this heat leak vanished when the fill line pressure fell below 100 microns. This cut-off pressure appeared to be very sharp, as determined by the change of slope of the heating curve of the calorimeter when it was far below T_λ during pump-out of the line. Normally the fill line was evacuated to well below 50 microns during measurements.

Results with the brass calorimeter: Heat capacity measurements were made along the vapour pressure curve over the range $-1.5 \times 10^{-5} < T - T_{\lambda} < 2.3 \times 10^{-5}$ deg with primary emphasis on the region within 2 microdeg. of T_{λ} . In this region the time constant for heat transfer from the calorimeter into the sample was less than 1 sec. Measurements were made by differentiation of the thermometer output under conditions of heating or cooling with constant power input using scanning rates between 1 and 9×10^{-8} deg/sec.

All temperature measurements were made relative to T_{\max} , the point of heat capacity maximum, which could generally be determined to within $\pm 2 \times 10^{-8}$ deg. The determination of this point and the perturbing effects of the isolation stage servo were the primary factors limiting the accuracy of the measurements.

Figures 3 and 4 show the data on linear temperature scales. The data are divided into three groups. Figure 3 shows the data in group 1 which are absolute measurements obtained from three heating and four cooling scans through the transition at rates between 4 and 9×10^{-8} deg/sec. Also shown for comparison is the tabulated data of Ahlers³. We have adjusted all our data by 4 J/mole deg to obtain better agreement with that of Ahlers. This quantity is within the uncertainty in the heat capacity of the empty calorimeter. The data in group 2 was obtained at rates between 2 and 6×10^{-8} deg/sec and were fitted to group 1 at two points 1.5 microdeg from T_{\max} . The data in group 3 were obtained at rates between 1 and 2 at 0.5 microdeg from T_{\max} . Data from all three groups within 1 microdeg of T_{\max} are shown in Figure 4. Detailed inspection of the data overlap away from the tie points showed no sign of systematic deviations between the groups, except possibly for group 1 within 0.1 microdeg of T_{\max} . Data from this group within 0.1 microdeg of T_{\max} was rejected, primarily because of the increasing uncertainties in the differentiation in this region.

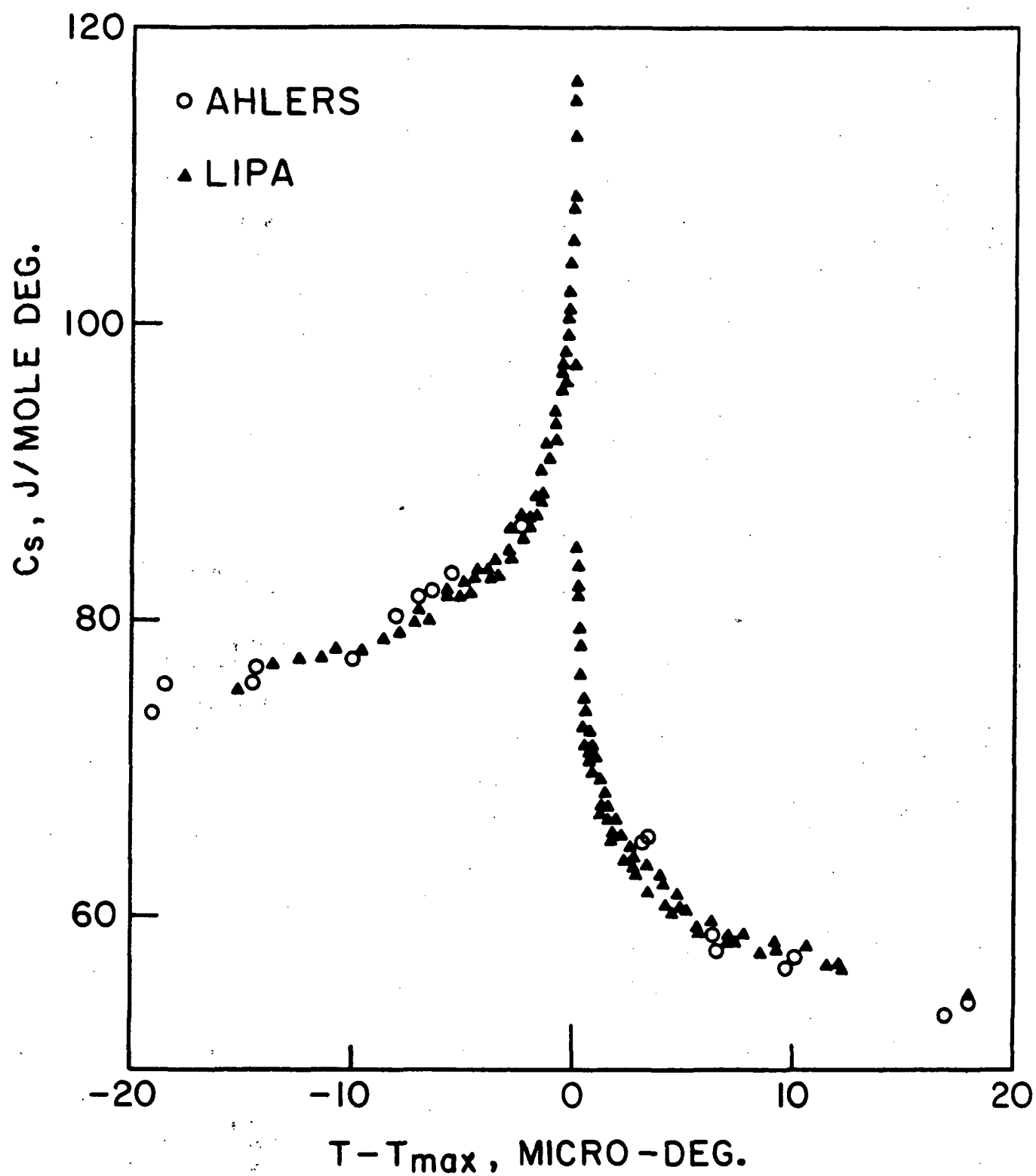


Figure 3: Wide range heat capacity measurements near the λ -point. Open circles are the measurements of Ahlers.

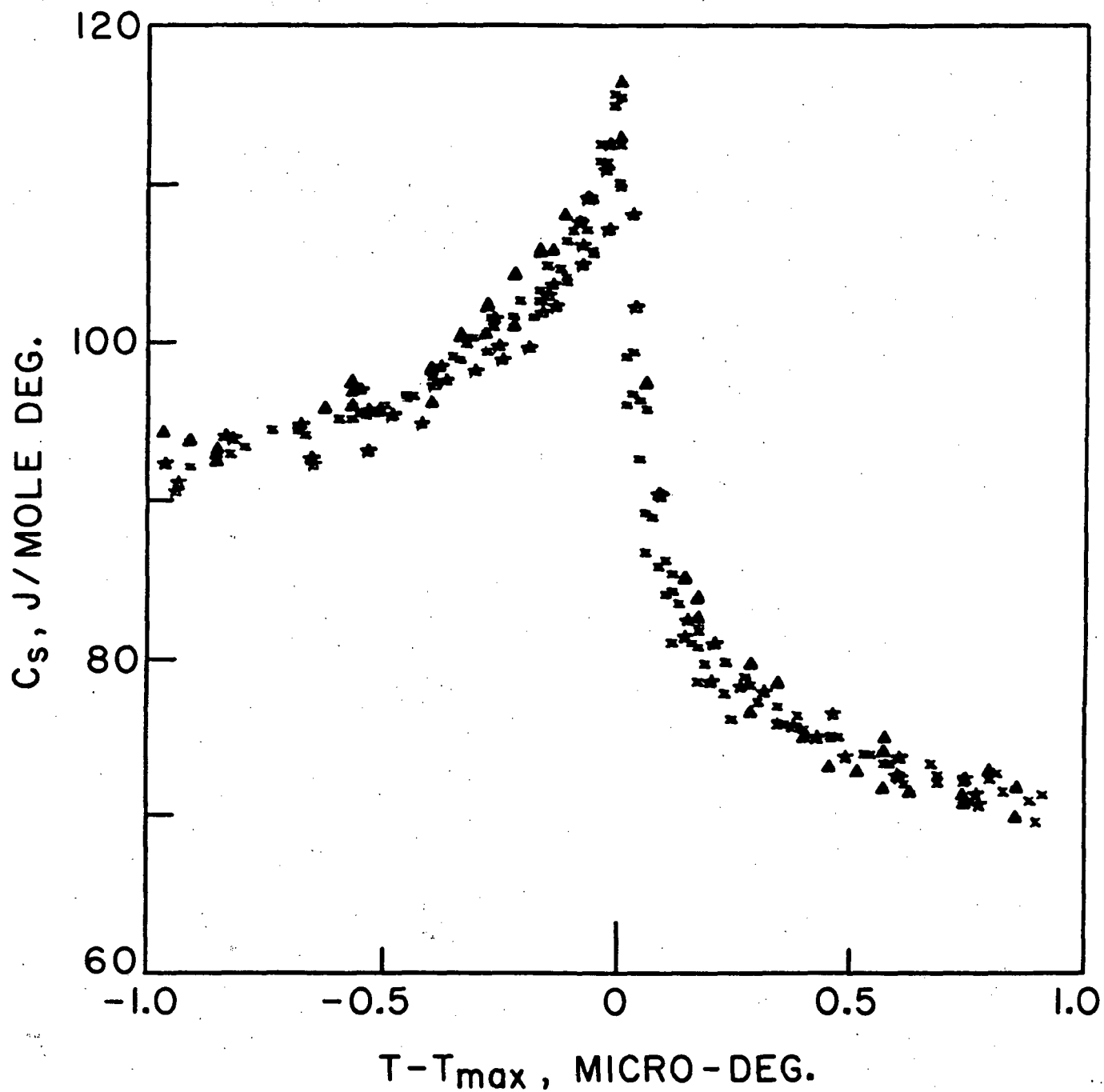


Figure 4: Preliminary heat capacity data obtained very close to the λ -point

Very close to the λ -transition gravitational effects cause a distortion of the heat capacity curve. The primary effect is to displace the maximum of the curve from T_λ by an amount proportional to the height of the sample. In our case this displacement is about 43 nanodeg. In addition, a correction term for gravitational averaging of the heat capacity can be calculated. In Figure 5 we plot the data corrected for the effect of gravity on a logarithmic temperature scale. The data below T_λ was cut off immediately below T_{\max} because of the sharp increase in the gravity correction at this point. On the high temperature side this feature is absent and we are limited primarily by our ability to locate T_{\max} .

From Figure 5 we can see that our data is in good agreement with that of Ahlers.³ On the other hand, extrapolation of a logarithmic function fitted to Ahlers' data does not fit our data well for $|t| < 10^{-7}$, especially below T_λ . Some improvement can be obtained by adjustment of T_λ relative to T_{\max} , but a good fit cannot be obtained simultaneously for the two branches of data. Apart from the small effect mentioned above, we find no systematic differences between heating and cooling data over the whole range of scanning rates.

The curvature of the data shown in Figure 5 is such that a small positive value of α is indicated, rather than the slightly negative value, $-.016 \leq \alpha \leq -.026$ found in a number of earlier experiments further from T_λ . Since the effect is only visible when our data is combined with that of Ahlers, we felt it important to establish the reality or otherwise of the effect in a single experiment with only one set of calibration constants, and preferably with no internal data adjustments. Since we had also noticed some non-equilibrium effects near T_λ at the higher heating rates which appeared to be due to temperature gradients in the calorimeter, we decided to conduct further

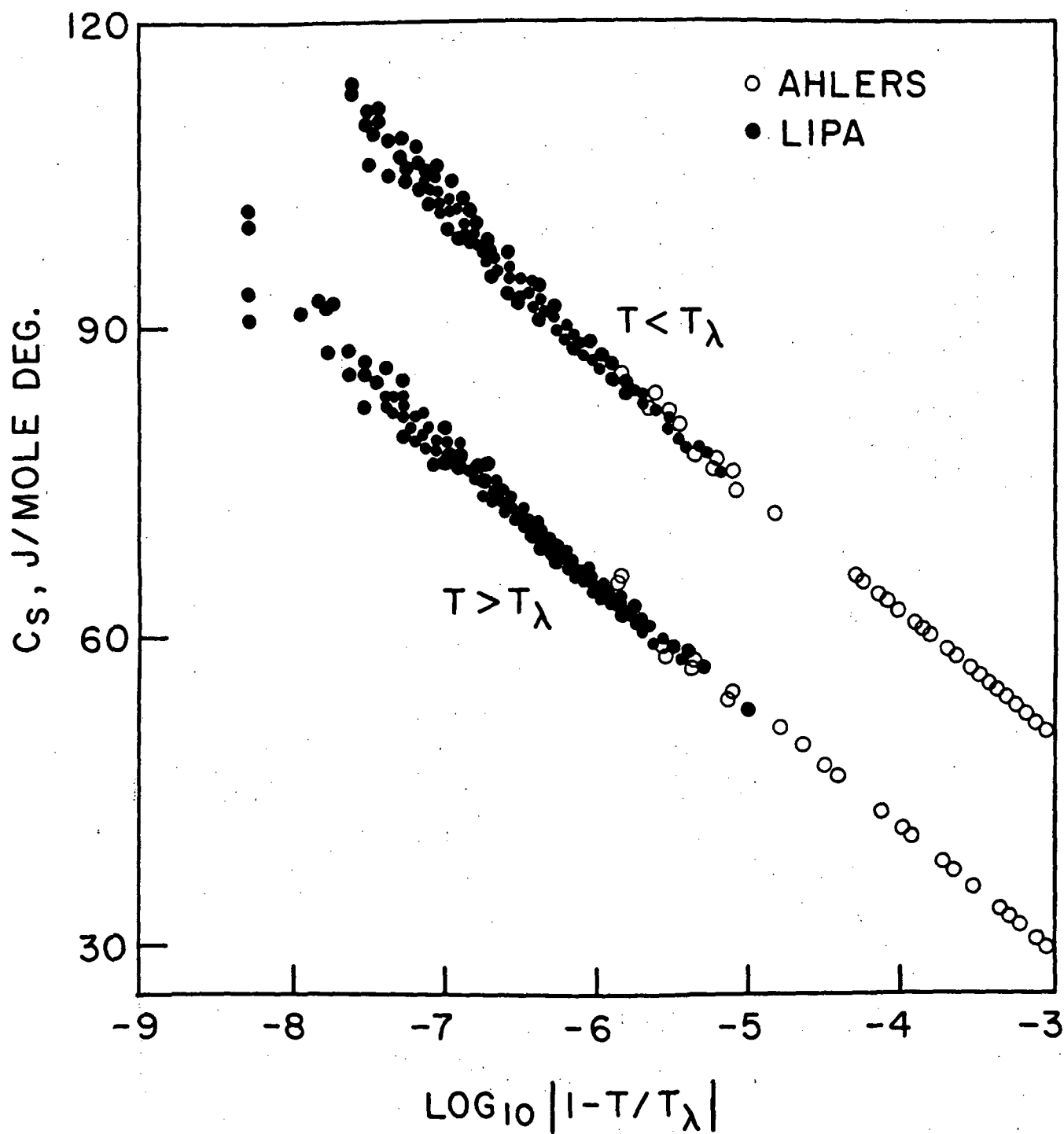


Figure 5: Log-linear plot of preliminary set of heat capacity data. Open circles are the measurements of Ahlers.

experiments using a copper calorimeter. The results of these measurements are described below. Before we leave the discussion of the preliminary results, we note that further analysis of the data conducted after the measurements described below, disclosed some additional heating rate dependence that had been overlooked in the first analysis. This effect is not very apparent due to the poor signal to noise ratio, but becomes more clearly visible with additional averaging and comparison with later measurements.

Results with the copper calorimeter: In this experiment improved control over the heat leak to the calorimeter was obtained by modifying the shielding of the sensing circuit for the HRT. Previously, a thick-walled lead tube was used between the HRT and the SQUID, thermally anchored at the isolation stages. A new tube was made from thin-walled niobium, drawn down to the niobium i.d. that would comfortably take the pick-up loop leads, about 0.15 mm. Also a distributed heater consisting of six metal film resistors evenly spaced around the base of the sample was installed to decrease temperature gradients. All important structural components were fabricated from OHFC copper. Data collection procedures were also improved, with the introduction of a digital system capable of reading the analog SQUID output signal with adequate signal/noise ratio. Software was developed to perform the differentiation and inversion of HRT output, and to convert the information to absolute heat capacity values. Figures 6 and 7 show the data on similar temperature scales to those in Figures 3 and 4 respectively. In the present figures three sets of data have been averaged, reducing the density of points and improving the signal to noise ratio. The most obvious feature of the new data is the lower peak height. Experiments described in the next section using completely new apparatus have verified this feature, as have numerous other scans through the transition not shown here. Since the heating rates were comparable to those in

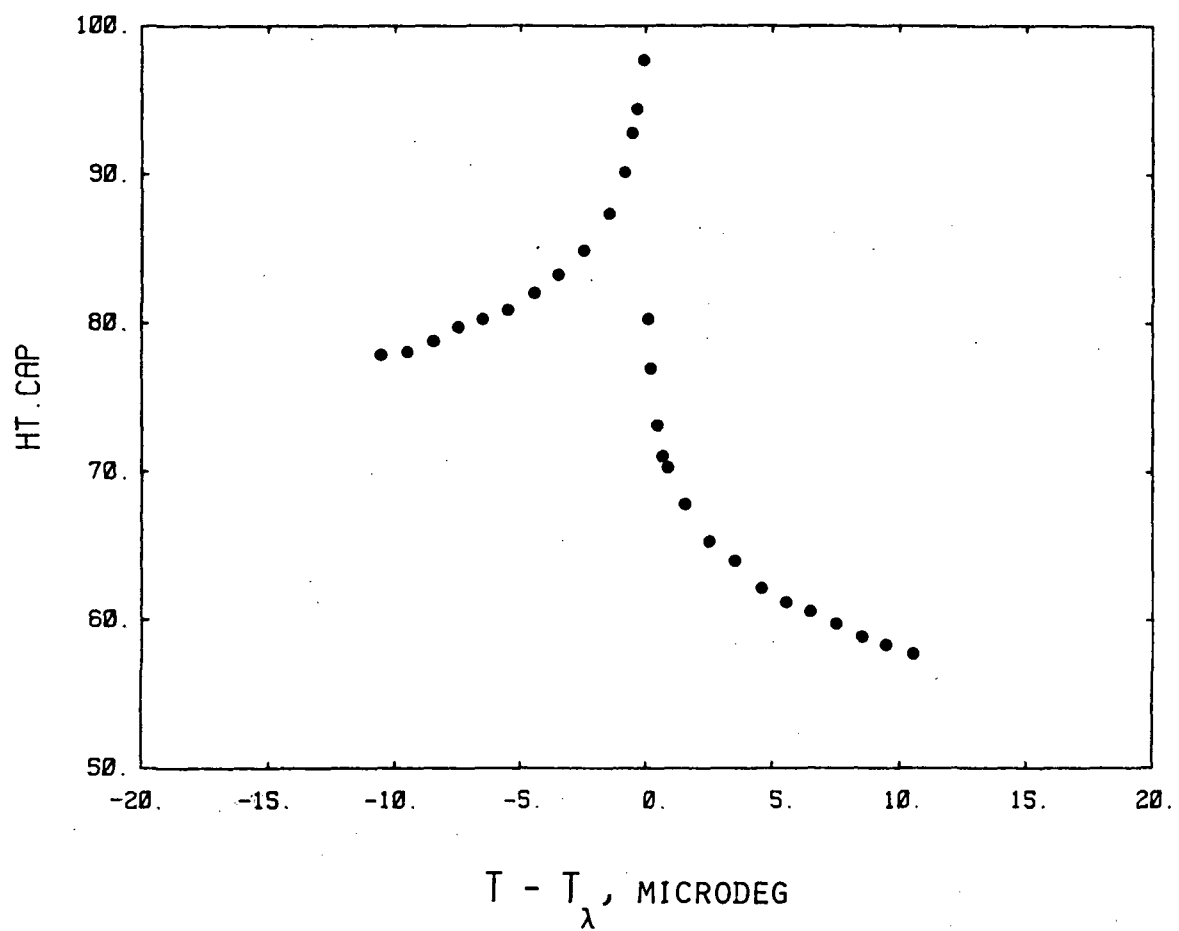


Figure 6: Heat capacity measurements over a wide range obtained with the copper calorimeter in the small thermal control system.

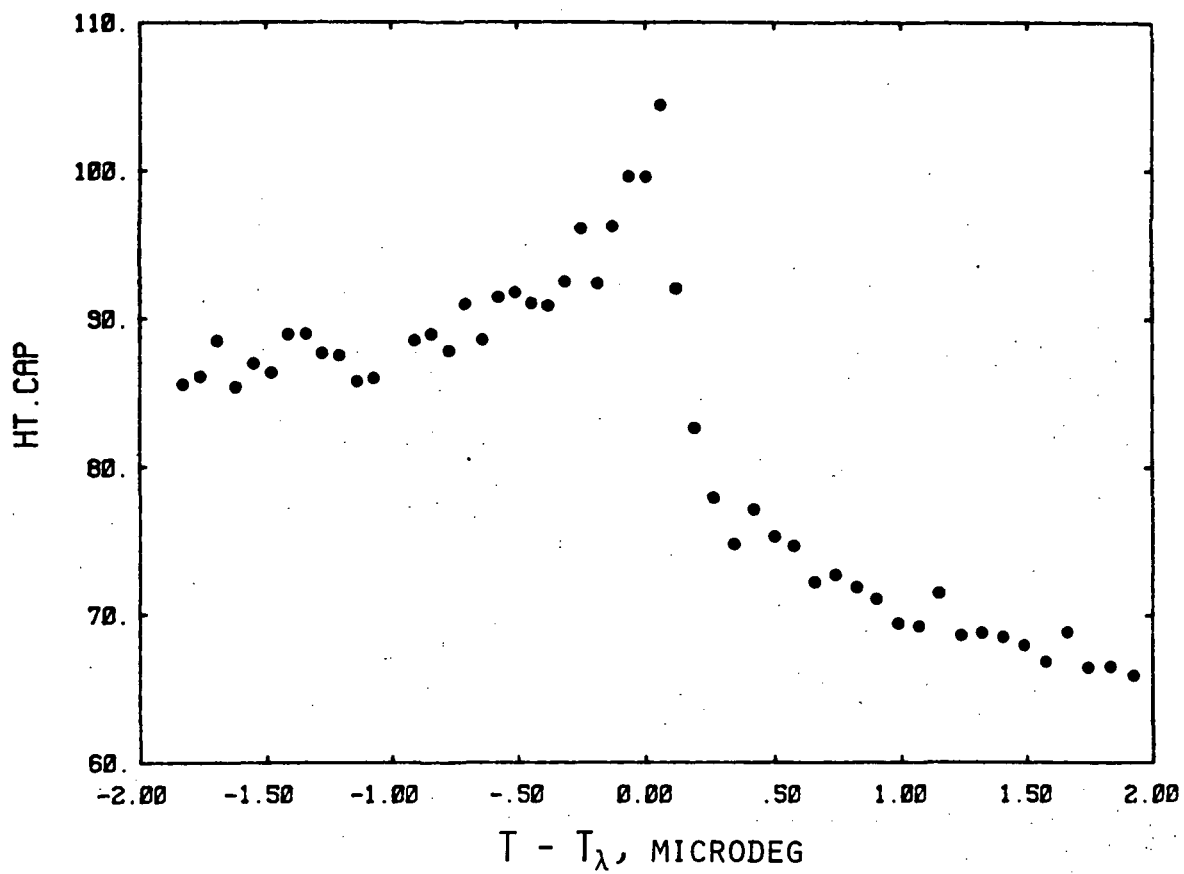


Figure 7: Narrow range measurements obtained with the copper calorimeter in the small thermal control system.

of the exponent. However, we found that the new data alone was insufficient to set useful bounds on the value of α due to the limited range available and relatively poor signal-to-noise ratio. We concluded that the best way to rectify these deficiencies was to build an improved thermal control system. This phase of the work and the results obtained with it are described in the following section.

In Figure 8 the data is plotted on a semi-logarithmic scale. It can be immediately seen that there is no longer a systematic curvature indicating a small positive exponent α . This is related to the reduction in the peak height mentioned above, but obviously now extending some distance below T_λ . The exact cause of this difference is not known since we did not attempt to corrupt the experiment in any way. We conjecture that the gradient effect is the most likely source of the distortion in the first data set. Later observations in the new apparatus described below showed that at high heating rates the distortion of the peak with the copper calorimeter is significantly less than with the brass. A possible additional source of the change may have been improved evacuation of the calorimeter fill line. In the initial experiments partial blockage of this line sometimes occurred due to condensible impurities in the helium sample. This effect may have led to erroneous estimates of the pressure in the low temperature section of the line. For the experiments in this and later sections, this problem was eliminated by improved trapping and gas handling procedures.

From the new data we conclude that the possible small positive value of α suggested by the preliminary measurements is a spurious effect, probably due to the presence of temperature gradients in the calorimeter. When this effect is reduced the data are entirely consistent with previous estimates

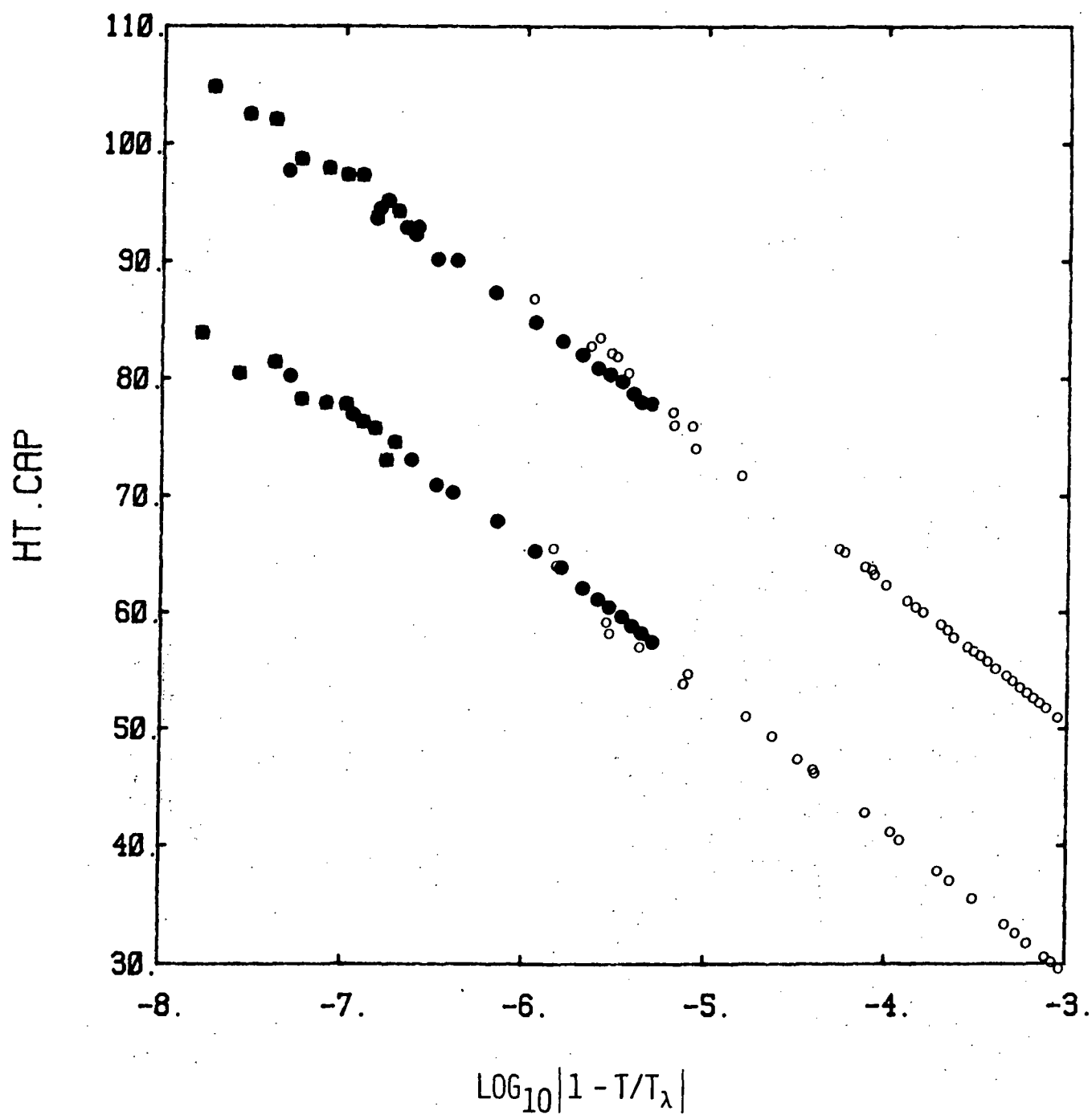


Figure 8: Log-linear plot of heat capacity data. o: measurements of Ahlers; ●: present experimental results with copper calorimeter

the previous experiment, temperature gradients in the apparatus were expected to be at least a factor of 30 lower through the use of copper in place of brass. Another aspect of the new data attesting to its improved quality is the absence of any need to adjust the baseline of the measurements to fit to previous experiments, or to internally adjust groups of data to improve consistency. This is due to improved heat leak control and knowledge of the total power switched at the end of each sweep through the transition.

IV. ADVANCED MEASUREMENTS

While the results described in the previous section represented a major advance in our knowledge of the heat capacity singularity at the λ -point, it was clear that significantly better measurements could be made with an improved apparatus. The limitations of the existing system were primarily due to the short (~8 hr.) time between helium transfers, which disrupted measurements and caused loss of thermal stability, and poor heat leak control due to the use of low resolution thermometers in the thermal control system. We therefore designed and built an improved apparatus described below, and used it to perform new measurements on two helium samples of different heights, 3 mm and 0.3 mm. This data has given rise to the best determination of the exponent α to date, and of course extends about two orders of magnitude closer to the transition than previous measurements, probing the asymptotic region much more effectively. The first set of results has been published in Physical Review Letters, and a paper describing the complete set of results is in preparation. We found that the value obtained for α is closer to the theoretical prediction than was observed previously further from the transition, indicating the possible existence of slow transients which perturb the representation of the singularity further from the λ -point.

Thermal Control System: One of the most desirable features of the new control system was the addition of a second HRT to control the heat leak to the calorimeter. However, since we were not sure that we could gain full advantage of this step simply by adding a thermal anchoring ring attached to a HRT, we also added a complete radiation and gas condensation shield between this new isolation stage and the continuously pumped cold stage. Another important feature was to move the system to a long-hold-time dewar, which increased our ability to continuously collect data by almost an order of magnitude. This change also had the advantage of increasing the maximum diameter of the system from 4 inches to 8 inches, greatly facilitating construction and the housing of multiple thermometers. Figure 9 shows a schematic view of the new thermal control system. The first stage of isolation inside the 4.2° K vacuum can is held in the range 1.6 to 2° K by a continuously pumped cold plate, similar to the one used in the earlier system. Stage 2 is the radiation and gas condensation shield surrounding the calorimeter and stabilized to within a few microKelvins with a germanium thermometer and integrating servo loop. Inside this shield is another stage of isolation consisting of a copper ring controlled to within a few nano-Kelvins with a HRT and another servo loop. All feedthroughs to the calorimeter stage are anchored to this ring. This system is capable of giving two to three orders of magnitude higher thermal stability for the calorimeter than was available previously. In operation we found it to be entirely adequate for our measurements, removing the issue of heat leak uncertainty from the area of our major concerns. In our most recent series of measurements, the thermal control system has been somewhat modified to include a servo-controlled thermal platform for mounting the SQUID sensors for the HRT's. This has improved the signal/noise ratio significantly, decreasing the time needed to obtain data of a given precision and resolution.

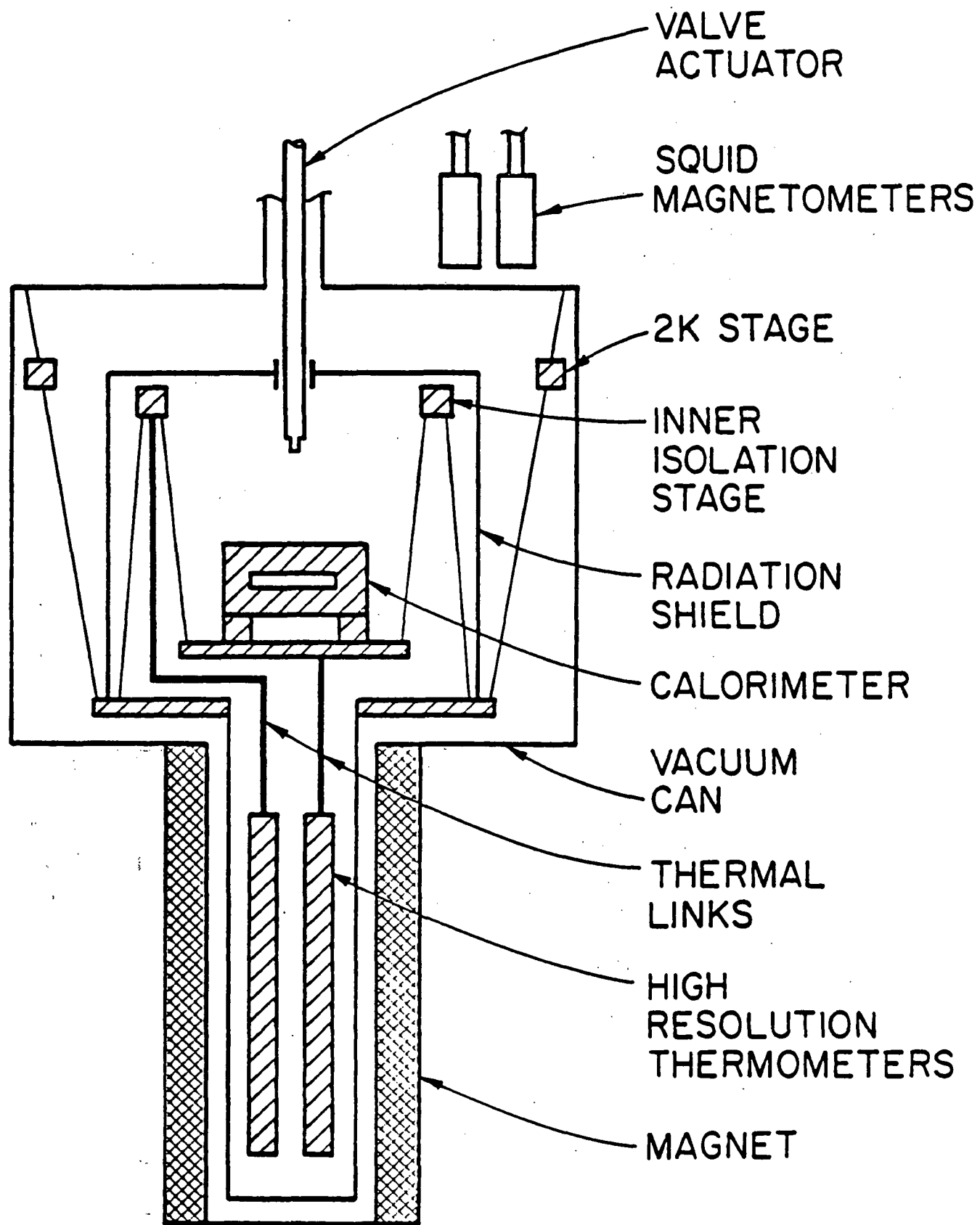


Figure 9: Schematic view of large thermal control system.

New Heat Capacity Measurements: With the new control system the main emphasis was initially placed on studying the heat capacity singularity of a 3 mm high sample of helium. This sample height was chosen because the finite size effects were expected to be negligible at least for $t > 3 \times 10^{-8}$, and the gravity corrections, while quite large, were still easily calculable. These measurements have been well described in Physical Review Letters 51, 2291 (1983) by J. A. Lipa and T. C. P. Chui, a copy of which is attached. For reference we have reproduced the data from the publication in Figures 10 and 11. We obtained a new value for α , $-0.0127 \pm .0026$ (2σ), which can be compared with the previous best value of $-.026 \pm .004$ obtained along the λ -line, and the theoretical prediction of $-.007 \pm .006$. Thus our measurement is in marginal agreement with theory but differs noticeably from the previous generally accepted value. A search of the literature discloses a number of independent experimental values for α which we have summarized in Table 2. It can be seen that our result for α is consistent with other measurements at the saturated vapor pressure, but that all measurements at higher pressures and along the ^3He - ^4He λ -line give somewhat more negative values, in the range $-.024$ to $-.026$. At face value, this situation implies a possible violation of the universality hypothesis which states that the exponent α is independent of pressure and ^3He concentration. However, a more likely explanation is that the previous experiments do not extend closely enough to the transition to give the asymptotic exponent because the confluent singularity correction terms are not properly accounted for. In either case, more definitive experiments are called for, and the solution will lead to a re-evaluation of the theoretical predictions for the λ -line.

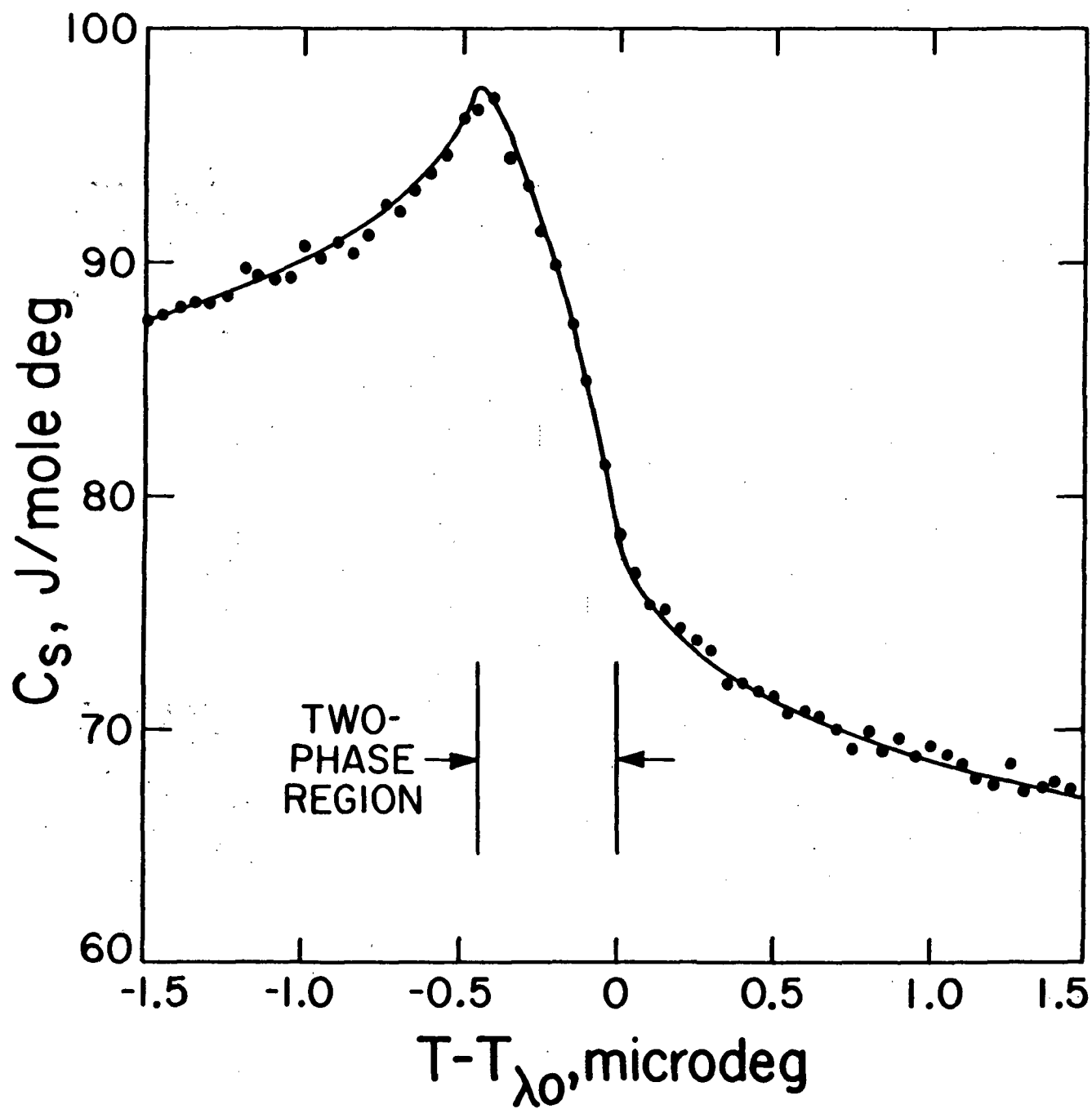


Figure 10: Heat capacity measurements with the 3 mm deep calorimeter in the vicinity of the two-phase region. Solid line shows the calculated gravity rounding.

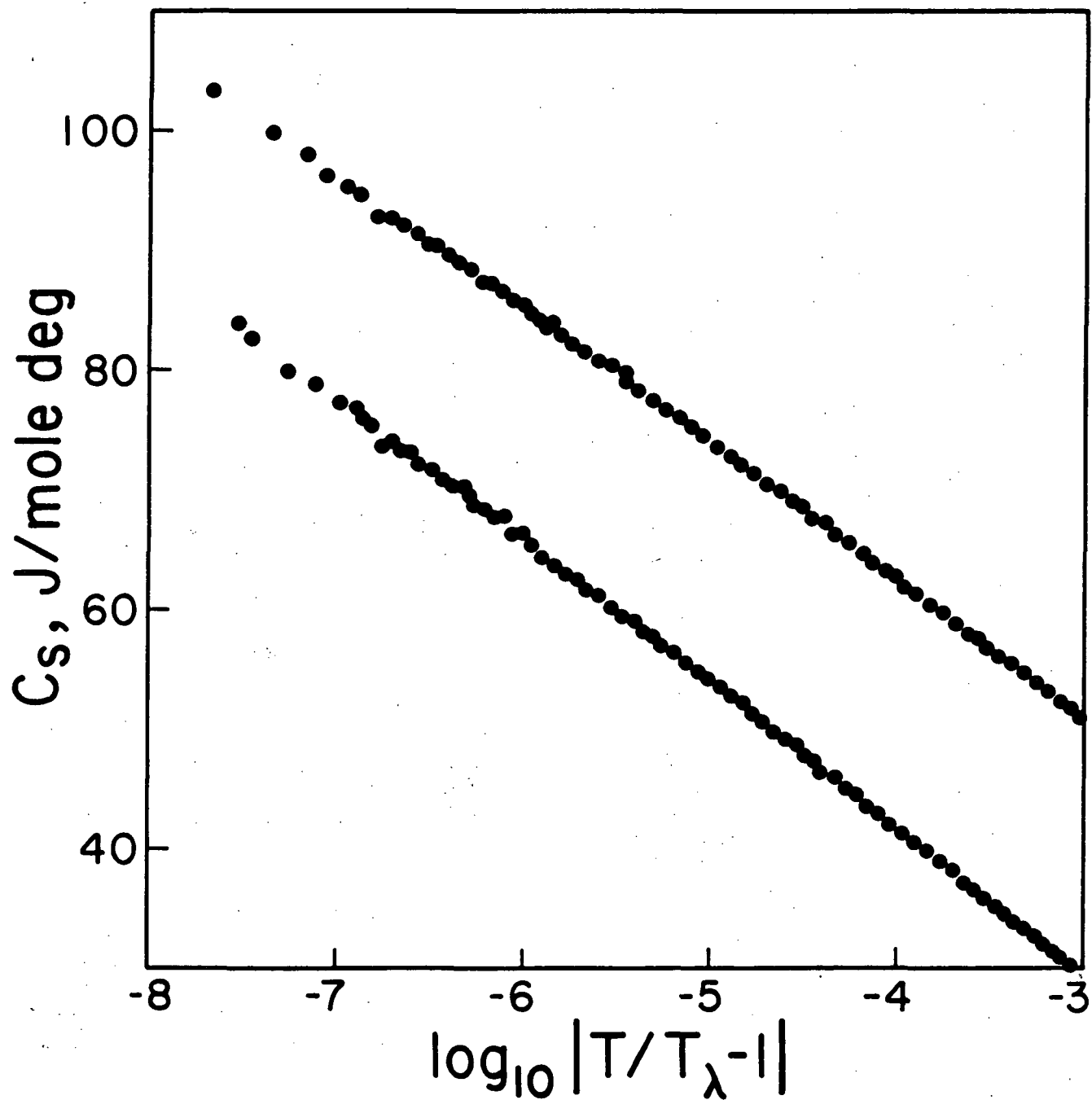


Figure 11: Log-linear plot of the heat capacity measurements over a wide range of temperature with the 3 mm calorimeter.

Table 2: Experimentally observed values of the heat capacity exponent α at the λ -point

Group	Parameter	α
BF & K	C_{Sat}	$0.0 \pm .05$
Ahlers	C_{Sat}	$0.000 \leq \alpha \leq -.026$
Ahlers	C_{Sat}	$-.0163 \pm .0017$
MAP	expansion coefficient	$-.026 \pm .004$
G & M	C_{Sat}	$-.0198 \pm .0037$
G & M	Mixtures	$-.025$
T & W	C_{Sat}	$-.017$
T & W	Mixtures	$-.024$

Very recently, C. Bagnuls and C. Bervillier⁹ have compared our data above T_λ with a new non-linear RG formulation of the heat capacity singularity which is expected to incorporate the confluent singularity term with fewer free parameters. When their model is fitted to our data, systematic departures are seen for $t > 7 \times 10^{-5}$. This is much closer to T_λ than $t \sim 10^{-3}$, the value obtained with the original model, and indicates that the confluent terms are not well controlled. Indeed, they find that to obtain agreement out to $t \sim 10^{-3}$ it is necessary to include two more terms in the expansion of the confluent series. This results in an increase in the number of parameters determined by fitting to the data over the number in the original RG model, making it even more difficult to obtain a meaningful test of the theory.

Since the experiment on the 3 mm sample was completed we have been able to improve the signal/noise ratio by a factor of about four. We decided to make use of this gain to study the heat capacity curve of a 0.3 mm high sample. In this case one would expect to see some additional rounding due to finite size effects superimposed on the gravity effect. In Figure 12 we show the results of our initial measurements on this sample. It should be noted that the temperature scale for this figure is ten times higher resolution than that in Figure 10. As expected, additional rounding is seen, and experiments were conducted to rule out the possibility of an experimental artifact. The most important test was to be sure that the rounding was independent of heating rate, which was found to be true for at least a factor of two change, both when heating and cooling. Also the possibility of inadvertent sample tilt leading to an enhanced gravity effect was explored without leading to any sharpening of the peak.

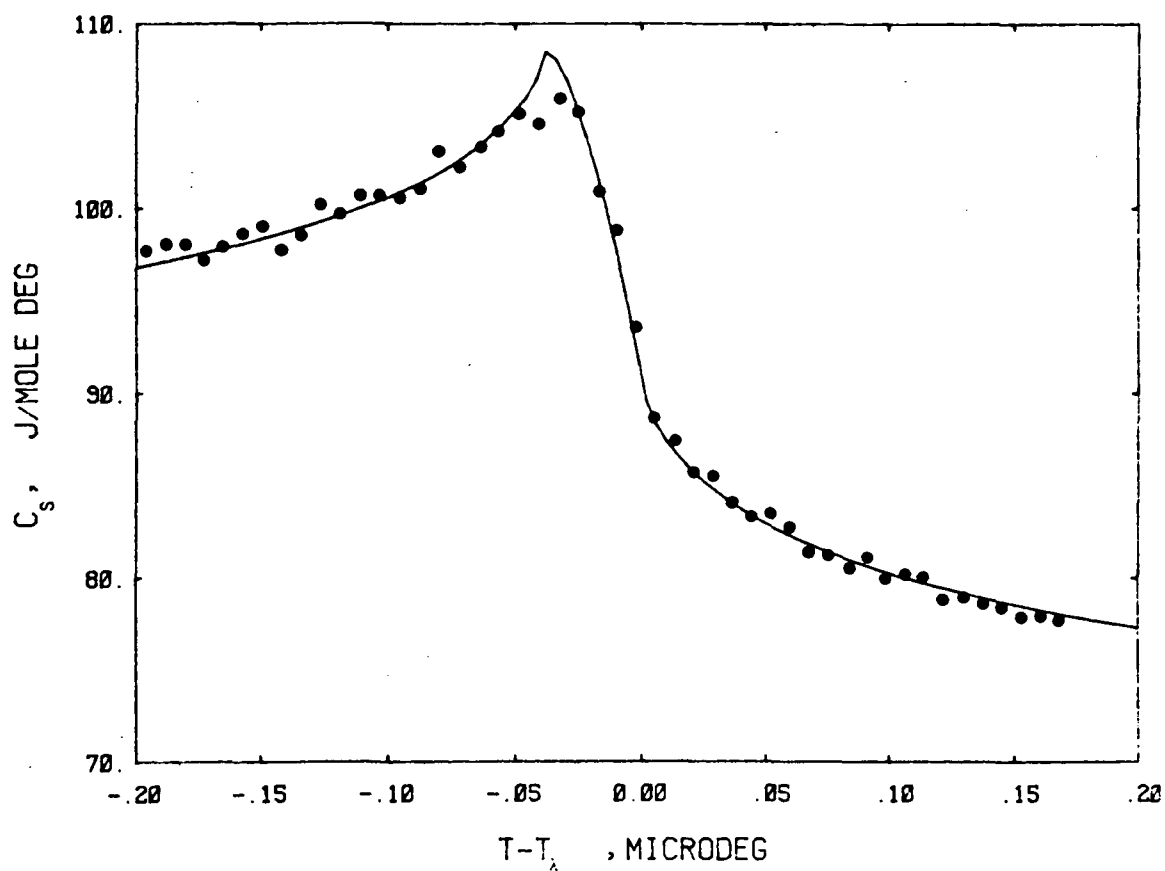


Figure 12: Heat capacity measurements with the 0.3 mm high calorimeter over a very narrow temperature range. Note that all data on this figure is within $t = 10^{-7}$. Solid line shows expected gravity rounding.

To test whether the gravity corrections applied to the 3 mm sample are reasonably accurate, we calculated the expected gravity rounded curve for the 0.3 mm sample using the best fit parameters from the first sample. We obtained an excellent fit to the new data as can be seen from Figure 13 in which both sets of data are plotted on the same scale. By the time this work was completed, all funds had long since been exhausted. Analysis of this data is continuing under separate funding and a new comparison with theory is expected shortly. With higher precision data it is extremely important to minimize the effect of systematic errors in the results which might introduce a temperature dependent curvature into the data. In this regard the linearity of the temperature scale and the corrections for the background heat capacity are of major importance. Extra care is being taken to understand and adequately allow for these effects before the analysis is taken to completion.

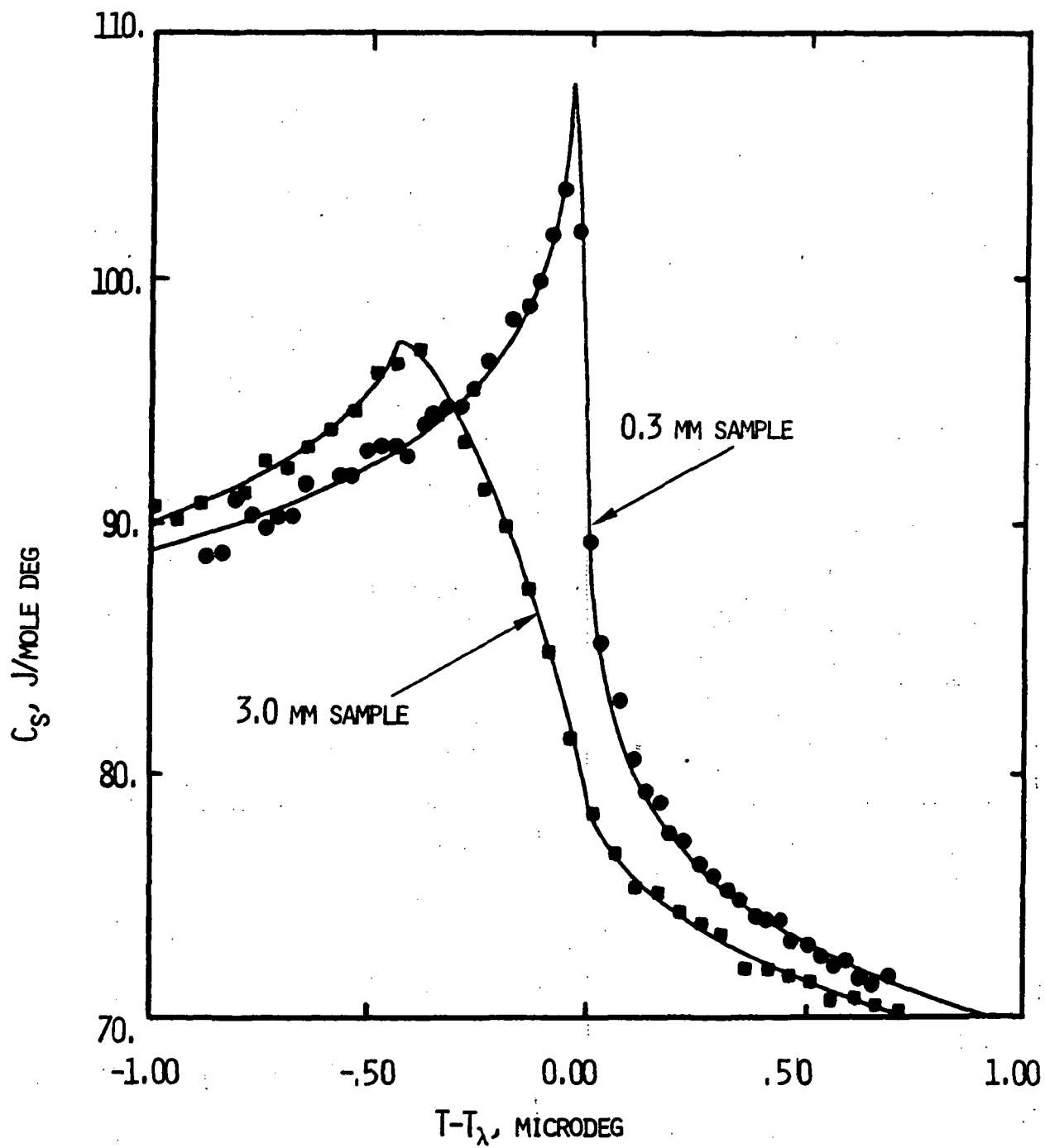


Figure 13: Comparison of data from 3 mm and 0.3 mm samples

REFERENCES

- 1) J. C. Le Guillou and J. Zinn-Justin, Phys. Rev. B21, 3976 (1980).
- 2) K. J. Mueller, G. Ahlers and F. Pobell, Phys. Rev. B14, 2096 (1976).
- 3) G. Ahlers, Phys. Rev. A 3, 696 (1971).
- 4) D. S. Greywall and G. Ahlers, Phys. Rev. A 7, 2145 (1973).
- 5) F. M. Gasparini and M. R. Moldover, Phys. Rev. B 12, 93 (1975).
- 6) G. Ahlers, Physica 107B, 347 (1981).
- 7) T. Takada and T. Watanabe, J. Low Temp. Phys. 41, 221 (1980).
- 8) F. M. Gasparini and A. A. Gaeta, Phys. Rev. B 17, 1466 (1978).
- 9) C. Bagnuls and C. Bervillier, preprint, 1984.

APPENDIX A

THE HEAT CAPACITY OF LIQUID HELIUM NEAR THE LAMBDA TRANSITION

Data Release #1; 1-15-84

J. A. Lipa and T. C. P. Chui
Physics Department, Stanford University
Stanford, Calif. 94305

Heat capacity measurements obtained with a sample of helium approximately 3 mm high at the saturated vapor pressure are given in Tables 1 and 2. The data has been corrected for the effect of gravity using method 3 described in Phys. Rev. Lett. 51, 2291 (1983). The present listing differs slightly from that used in the above article due to some minor changes in the data averaging near T_λ . However, the results of curve fitting are virtually identical. The data is plotted on a log-linear scale in Fig. 1. Using the functional form

$$C_s = (A/\alpha) t^{-\alpha} (1 + Dt^{0.5}) + B ; \quad t = |1 - T/T_\lambda| ;$$

the data can be adequately represented with the following parameter values:

$$\begin{aligned} \alpha (= \alpha') &= -0.013 \\ A &= 6.108 \text{ J/mole deg} \\ A' &= 5.771 \quad " \\ B &= 458.42 \quad " \\ B' &= 456.05 \quad " \\ D &= -0.022 \\ D' &= -0.020 \end{aligned}$$

It should be noted that far from T_λ , possible spurious linear terms may exist in the data amounting to of the order 0.1% at $t \sim 10^{-3}$ due to uncertainties in the thermometer calibration and the calorimeter heat capacity. These effects are still under investigation: a further data release is planned for the near future.

ORIGINAL PAGE IS
OF POOR QUALITY

Table 1

Heat capacity vs. temperature above the λ -point. Temperature units: micro-deg; heat capacity units: Joule/mole degree. The heat capacity data has been corrected for the effect of gravity.

$T-T_{\lambda}$	C_s	$T-T_{\lambda}$	C_s	$T-T_{\lambda}$	C_s
.075	82.04	4.174	62.48	97.077	46.04
.080	82.97	4.522	61.81	104.933	45.42
.120	79.80	4.922	61.48	115.293	44.90
.153	79.88	5.278	61.33	125.213	44.61
.175	77.96	5.720	60.76	134.983	44.55
.198	78.96	6.195	60.20	145.923	43.59
.221	77.26	6.677	60.00	155.253	43.53
.247	76.68	7.188	59.51	163.423	43.03
.275	76.29	7.649	59.55	178.953	42.54
.298	76.79	8.421	59.09	194.673	41.90
.323	74.67	9.011	58.41	211.343	41.75
.349	75.51	9.676	58.07	228.753	41.10
.374	73.90	10.547	57.73	243.503	40.91
.411	73.77	11.483	57.02	261.703	40.57
.472	73.47	12.498	56.87	279.533	40.40
.522	72.96	13.441	56.26	306.093	39.97
.573	72.26	14.471	56.37	334.873	39.33
.623	71.76	15.590	55.72	360.453	38.87
.672	71.59	16.515	55.17	384.363	38.58
.724	71.52	18.069	54.78	415.423	38.32
.785	70.78	19.555	54.47	449.943	37.77
.874	70.34	21.059	54.14	485.523	37.03
.975	69.92	23.045	53.48	521.233	36.98
1.075	69.58	25.065	53.45	564.833	36.51
1.149	68.80	27.073	52.95	615.043	36.02
1.274	68.31	29.028	52.52	660.133	35.69
1.341	68.32	31.013	52.40	715.433	35.13
1.472	67.60	32.756	51.77	769.513	34.81
1.546	67.80	35.728	51.29	829.673	34.45
1.695	67.90	38.854	50.59	895.843	33.97
1.827	66.19	41.785	50.54	969.163	33.59
1.955	66.34	44.761	50.10	1042.723	33.23
2.128	66.51	48.558	49.51	1130.123	32.79
2.320	65.86	52.539	49.23	1220.223	32.44
2.494	65.43	56.225	48.88	1320.623	31.97
2.653	64.62	60.970	48.74	1432.723	31.52
2.884	64.16	66.580	47.83	1540.223	31.21
3.125	63.96	71.062	47.69	1656.523	30.79
3.309	63.73	76.702	47.36	1795.023	30.29
3.571	63.10	83.233	46.79	1935.223	29.94
3.878	62.80	89.778	46.68	2026.023	29.73

Table 2

Heat capacity measurements below the λ -point. Same units as Table 1.

$T-T_\lambda$	C_s	$T-T_\lambda$	C_s	$T-T_\lambda$	C_s
-.029	105.50	-7.788	78.77	-144.303	64.41
-.068	101.58	-8.543	78.61	-155.133	63.79
-.116	99.26	-9.230	77.59	-163.943	63.72
-.171	97.52	-10.055	77.52	-179.693	63.15
-.202	96.32	-11.066	77.19	-194.023	62.97
-.276	94.98	-12.028	76.85	-210.203	62.47
-.313	94.57	-13.001	76.47	-225.143	62.37
-.382	92.43	-14.012	75.98	-239.903	61.87
-.426	92.85	-15.050	75.93	-259.133	61.49
-.495	91.95	-16.057	75.61	-279.393	61.07
-.593	91.23	-17.511	75.04	-304.963	60.56
-.685	90.73	-19.100	74.59	-329.653	60.17
-.773	90.07	-20.255	74.41	-354.393	59.94
-.870	89.19	-22.521	73.39	-384.463	59.46
-.979	88.81	-23.559	73.64	-414.733	59.16
-1.094	88.54	-26.373	72.63	-449.353	58.56
-1.192	88.56	-28.497	72.75	-489.723	58.22
-1.335	87.21	-29.841	72.23	-524.603	57.72
-1.484	87.53	-32.664	71.72	-564.313	57.60
-1.646	86.46	-35.636	71.43	-613.993	57.08
-1.816	85.86	-38.565	70.97	-659.463	56.65
-1.943	85.60	-41.664	70.39	-710.363	56.14
-2.164	85.28	-44.937	70.28	-769.293	55.94
-2.394	84.68	-48.153	70.13	-829.313	55.54
-2.643	84.11	-51.631	69.33	-894.163	55.09
-2.821	83.40	-56.211	68.99	-969.403	54.79
-3.091	84.26	-61.374	69.08	-1049.543	54.23
-3.378	82.87	-66.078	68.48	-1133.943	53.95
-3.714	82.26	-71.293	67.88	-1224.543	53.45
-4.043	82.19	-76.533	67.69	-1319.843	53.12
-4.379	81.54	-83.048	67.20	-1424.443	52.64
-4.794	81.19	-89.597	66.90	-1539.343	52.32
-5.251	81.05	-96.186	66.36	-1664.443	51.98
-5.702	80.38	-104.773	65.95	-1794.743	51.57
-6.115	80.56	-115.493	65.61	-1934.143	51.10
-6.763	80.11	-124.543	65.12	-2084.543	50.65
-7.278	78.59	-134.213	64.43		

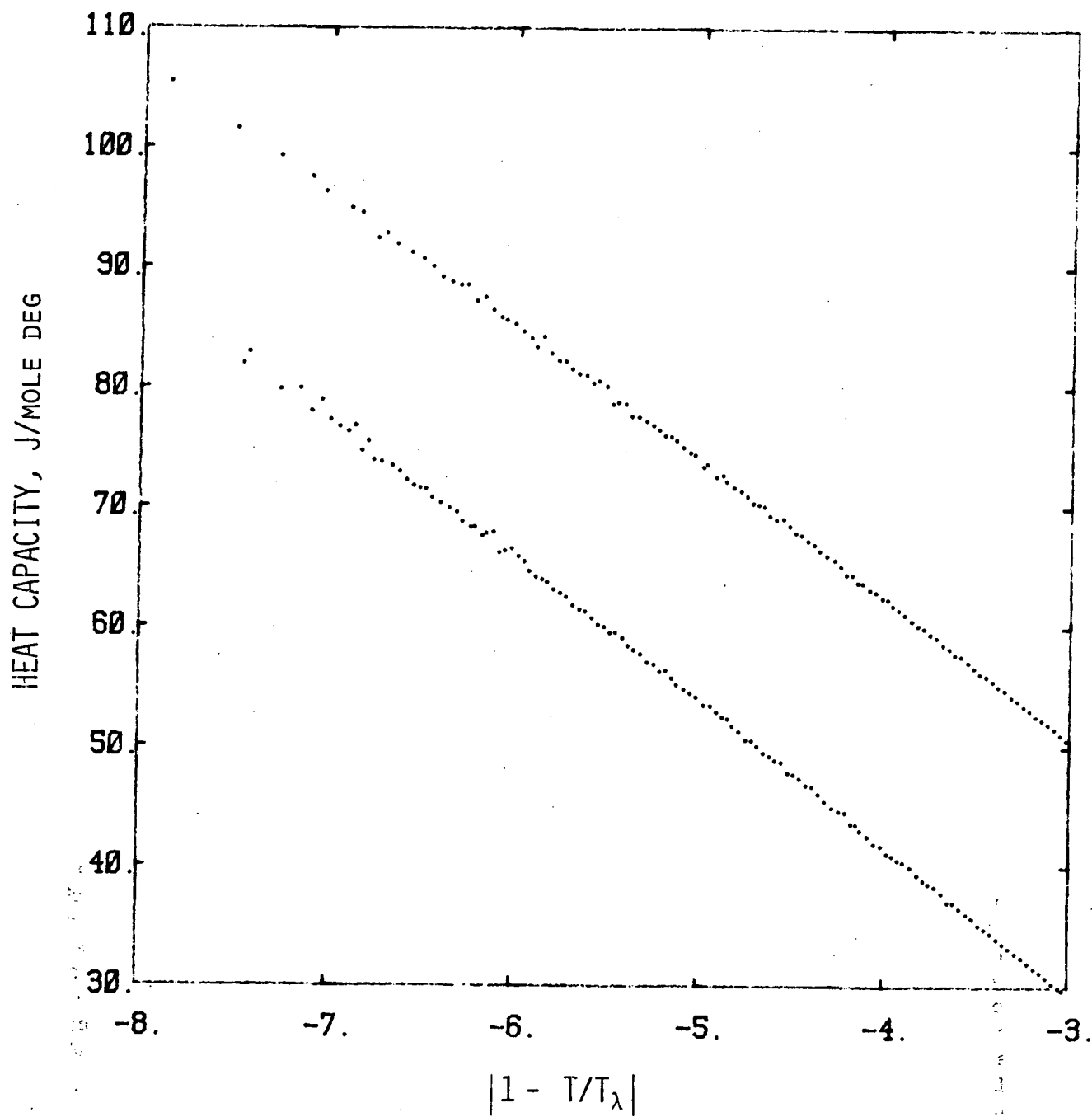


Figure 1

Temperature dependence of heat capacity near the λ -point plotted on a log-linear scale. The measurements have been corrected for the effect of gravity near T_λ .

HIGH RESOLUTION HEAT CAPACITY MEASUREMENTS NEAR THE LAMBDA POINT OF HELIUM*

J. A. Lipa

Physics Dept., Stanford University, Stanford, CA 94305

We report preliminary measurements of the heat capacity of a .03 cm high sample of helium over the range $|t| = 10^{-6}$ to 10^{-5} , where $t = 1 - T/T_\lambda$. The data is consistent with a logarithmic singularity in C_p , but with a somewhat higher coefficient than is found further from T_λ . When combined with other measurements¹ extending to $|t| = 10^{-4}$, the total data indicate a possible small positive value for the exponent α .

INTRODUCTION

One of the important results derived from the application of renormalization group techniques to the problem of co-operative transitions has been a clarification of the role of confluent singularities in the functional representation of the thermodynamic variables of a system.² Unless allowance is made for such secondary singularities, values of exponents may be perturbed. Frequently, however, this allowance can lead to a drastic reduction in the severity of experimental tests of theoretical predictions. One way to avoid this difficulty is to perform higher resolution measurements. We report some preliminary measurements of the heat capacity of liquid helium which extend about two orders of magnitude closer to the λ -transition than previous experiments.^{1,3} Our results indicate a slightly different divergent behavior than is found further from the transition. By themselves, the new measurements are consistent with a logarithmic singularity in C_p , but with a somewhat larger coefficient than was reported previously. When taken together with the data of Ahlers¹, they indicate a small but positive value for the exponent α , assuming no significant contribution from a confluent singularity for $|t| < 10^{-4}$.

APPARATUS

An 8 mg helium sample of vertical height .03 cm was sealed inside a thick-walled brass calorimeter using an all-metal valve that could be closed at low temperatures. The calorimeter was attached to a support structure and thermometer assembly by eight thick copper wires with anchor points distributed over its surface to minimize temperature gradients. Relative temperatures were measured using a paramagnetic salt thermometer⁴ with a resolution of about 6×10^{-10} deg in a 1 Hz bandwidth at the λ -point. The calorimeter was suspended from low thermal conductivity stainless steel supports inside a vacuum can located in the helium bath. All connections to the calorimeter were thermally anchored to an isolation stage servo-regulated with a control system using a carbon resistor sensor. The time constant for heat transfer between the calorimeter and its surroundings was about 3 hr.

OBSERVATIONS

Heat capacity measurements were made along the vapour pressure curve over the range $-1.5 \times 10^{-5} < T - T_\lambda < 2.3 \times 10^{-5}$ deg with primary emphasis on the region within 2 microdeg of T_λ . In this region the time constant for heat transfer from the calorimeter into the sample is expected to be less than 1 sec. Measurements were made by differentiation of the thermometer output under conditions of heating or cooling with constant power input using scanning rates between 1 and 9×10^{-6} deg/sec.

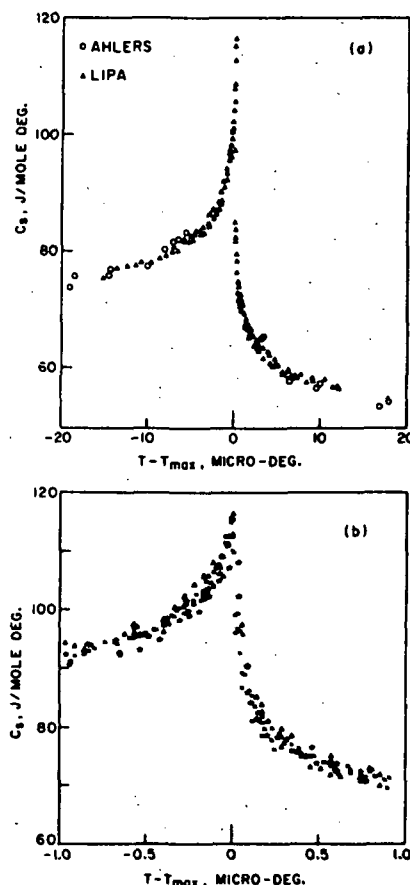


Figure 1: Heat capacity measurements close to T_λ on linear temperature scales.

All temperature measurements were made relative to T_{\max} , the point of heat capacity maximum, which could generally be determined to within $\pm 2 \times 10^{-8}$ deg. The determination of this point and the perturbing effects of the isolation stage servo were the primary factors limiting the accuracy of the measurements.

Figure 1 shows the data on linear temperature scales. The data are divided into three groups. Fig. 1(a) shows the data in group 1 which are absolute measurements obtained from three heating and four cooling scans through the transition at rates between 4 and 9×10^{-8} deg/sec. Also shown for comparison is the tabulated data of Ahlers.¹ We have adjusted all our data by 4 J/mole deg to obtain better agreement with that of Ahlers. This quantity is within the uncertainty in the heat capacity of the empty calorimeter. The data in group 2 were obtained at rates between 2 and 6×10^{-8} deg/sec and were fitted to group 1 at two points 1.5 microdeg from T_{\max} . The data in group 3 were obtained at rates between 1 and 4×10^{-8} deg/sec and were fitted to groups 1 and 2 at 0.5 microdeg from T_{\max} . Data from all three groups within 1 microdeg of T_{\max} are shown in Fig. 1(b). Detailed inspection of the data overlap away from the tie points showed no sign of systematic deviations between the groups, except possibly for group 1 within 0.3 microdeg of T_{\max} . Data from this group within 0.1 microdeg of T_{\max} was rejected, primarily because of the increasing uncertainties in the differentiation in this region.

Very close to the λ -transition gravitational effects^{1,5} cause a distortion of the heat capacity curve. The primary effect is to displace the maximum of the curve from T_{λ} by an amount proportional to the height of the sample. In our case this displacement is about 43 nano-deg. In addition, a correction term for gravitational averaging of the heat capacity can be calculated.⁵ In Fig. 2 we plot the data corrected for the effect of gravity on a logarithmic temperature scale. The data below T_{λ} was cut off immediately below T_{\max} because of the sharp increase in the gravity correction at this point. On the high temperature side this feature is absent and we are limited primarily by our ability to locate T_{\max} .

With a sample of small vertical height, distortion of the heat capacity curve due to finite size effects is expected very close to T_{λ} . The data of Chen and Gasparini⁶ indicate that these effects are significantly smaller than the gravity effects: we have ignored them for the present.[†]

From Fig. 2 we can see that our data is in good agreement with that of Ahlers.¹ On the other hand, extrapolation of a logarithmic function fitted to Ahlers data does not fit our data well for $|t| < 10^{-7}$, especially below T_{λ} . Some improvement can be obtained by adjustment of T_{λ} relative to T_{\max} but a good fit cannot be obtained simultaneously for the two branches

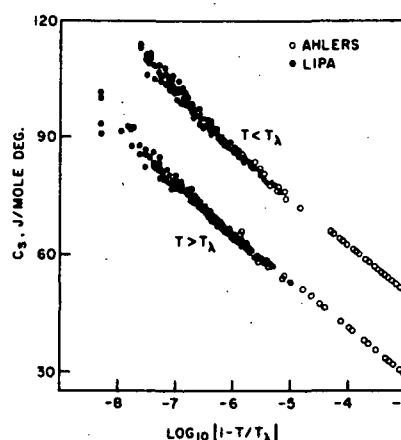


Figure 2: Log-linear plot of heat capacity data corrected for the effect of gravity.

of data. Apart from the small effect mentioned above, we find no systematic differences between heating and cooling data over the whole range of scanning rates. Since all gas lines to the calorimeter were continuously evacuated to below 50 microns pressure, it is unlikely that a superfluid thermal short exists in the system.

We conclude that some evidence now exists for a departure from the close-to-logarithmic divergence of C_p observed for $|t| > 10^{-6}$. While our data alone is consistent with a logarithmic singularity with a somewhat higher amplitude, when combined with the data of Ahlers, a slightly positive value for the exponent α is indicated. Experiments are continuing to clarify these issues.

FOOTNOTES

*: This work supported by NASA Contracts #NAG2-62 and #955057.

†: See, however, M. Archibald et al (Phys. Rev. Lett. 21, 1156 (1968)).

REFERENCES

- 1) G. Ahlers, Phys. Rev. A 3, 696 (1971)
- 2) M. Chang and A. Houghton, Phys. Rev. B 21, 1881 (1980)
- 3) M. J. Buckingham and W. M. Fairbank, in Progr. in Low Temp. Phys. (C. J. Gorter (ed), North Holland, Amsterdam (1961)) 3, 80
- 4) J. A. Lipa, B. C. Leslie and T. C. Wallstrom - submitted to these Proceedings.
- 5) C. F. Kellers, Thesis, Duke University, 1960
- 6) T. P. Chen and F. M. Gasparini, Phys. Rev. Lett. 40, 331 (1978)

Very High-Resolution Heat-Capacity Measurements near the Lambda Point of Helium

J. A. Lipa and T. C. P. Chui

Physics Department, Stanford University, Stanford, California 94305

(Received 5 July 1983)

New measurements of the heat capacity of a sample of helium 3 mm high are reported which extend to within 5×10^{-8} deg of the lambda transition at the vapor pressure. From an analysis of the results allowing for the effect of gravity, the values -0.0127 ± 0.0026 (2σ) for the exponent α ($=\alpha'$) and 1.058 ± 0.004 for the leading singularity ratio A/A' are obtained. These values are in closer agreement with the theoretical predictions than those reported previously.

PACS numbers: 65.40.Hq, 67.40.Kh

Experimental tests of the renormalization-group (RG) predictions¹ for cooperative transitions involve parameter estimation by curve fitting to data. The accuracy of the parameter values depends on the degree of distortion of the data due to sample defects, the measurement uncertainties, and the dynamic range of the independent variable. Near the λ transition of ⁴He at the vapor pressure, an exceptionally wide range of temperature is available extending from $t = |1 - T/T_\lambda| \sim 10^{-3}$ to $\sim 10^{-8}$, limited ultimately by the tradeoff between finite-size effects and gravitational rounding. This range is the maximum for any known cooperative transition and experiments on this system should therefore provide the best tests of theoretical predictions. Many experiments have been performed near the λ transition, but none have spanned the complete range of t available. In this paper we report heat-capacity measurements on a sample of helium 3 mm high which extend from $t = 10^{-3}$ to well inside the gravity-affected region. Previously we studied² the heat-capacity curve of a sample of height 0.3 mm. The present experiment was undertaken both to improve the quality of the measurements and to minimize those distortions of the heat-capacity curve which are less well understood, and which might perturb values obtained for quantities of theoretical interest. By increasing the sample height from 0.3 to 3 mm, finite-size effects and nonlocal contributions to the gravity corrections are reduced, but at the expense of a large increase in the gravity effect due to the finite slope of the λ line. In addition to causing a distortion of the heat-capacity curve, which can be easily calculated,³ this effect induces a two-phase region within the sample where both He I and He II coexist. For the present experiment the width of this region, δT_2 , is about 4×10^{-7} K. We corrected our data for the effect of gravity and then performed curve fitting to extract parameters for

comparison with the RG predictions. The exponent value we obtained agrees with theory better than the commonly quoted value,⁴ $\alpha = -0.026 \pm 0.004$, obtained along the λ line,⁵ and agrees well with previous measurements at the vapor pressure,^{3,6} made further from the transition.

A 270-mg helium sample was sealed inside an annular copper calorimeter with a low-temperature valve. The sample filled about 80% of the volume of the calorimeter to a uniform depth of 3 mm, the minimum dimension of the sample. The calorimeter was attached to a paramagnetic-salt thermometer described elsewhere.⁷ This assembly was installed in a multistage thermal enclosure shown in Fig. 1 and placed in a helium bath at 4.2 K. The first stage of thermal isolation was held at 1.6 K by a continuously pumped cold plate.⁸ The second stage consisted of a com-

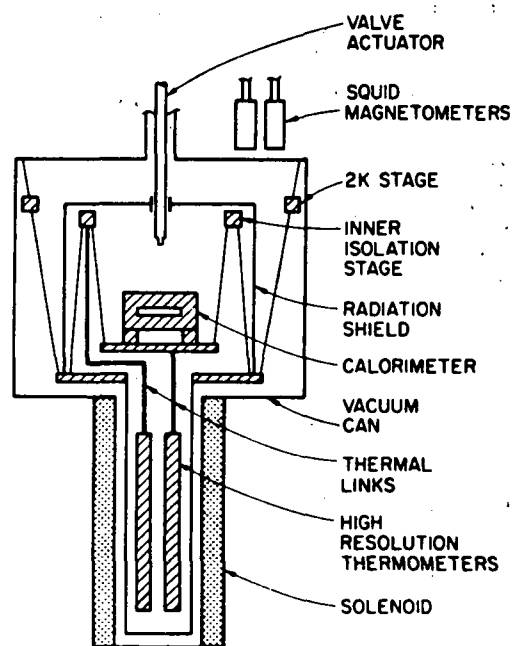


FIG. 1. Schematic view of thermal control system.

plete copper shield thermally controlled with a germanium thermometer and an integrating servo loop. The final stage was a copper ring which intercepted all connections to the calorimeter and was thermally controlled with a second paramagnetic salt thermometer.

Heat-capacity measurements were performed with use of a continuous heating (or cooling) method with constant power input. The thermometer signal as a function of time was digitally differentiated over periods from 5 to 80 sec to give heat-capacity information. Scanning rates were varied from 4×10^{-10} to 10^{-7} K/sec to search for nonequilibrium phenomena within the sample. In addition, during a measurement cycle the heater power was regularly stepped by a known amount to determine the background heat leak. At such times we observed the thermal response of the system by monitoring the associated transients. Within $0.5 \mu\text{K}$ of the transition the thermal response time was less than 8 sec, in agreement with values calculated from the thermal conductivity of the helium.⁹ For scanning rates below 1.5×10^{-9} K/sec we found no difference between data obtained while heating and while cooling. For rates up to 8×10^{-9} K/sec, the data in the two-phase region were displaced a few nanodegrees, depending on scanning rate and temperature. Data affected in this way were averaged with similar data obtained while cooling at a comparable rate. For higher rates, some smearing of the transition was observed, and all affected data were rejected. The main scale factor uncertainty in the measurements ($\pm 1.5\%$) was due to the determination of the sample mass. Temperature-dependent uncertainties in other scale factors were estimated to be less than 0.1% over the range of measurements. In Fig. 2 we show the data for rates below 3×10^{-9} K/sec on a linear scale in the vicinity of the two-phase region. Each data point is an average of about twenty independent measurements which fall in bins 5×10^{-8} K wide. The temperature scale has been plotted relative to the location of the λ transition at the gas-liquid interface, $T_{\lambda 0}$, which was determined in the curve-fitting procedure described below.

To estimate the exponents α and α' (below T_λ), and other quantities of theoretical interest, we fitted the data corrected for the effect of gravity by functions of the form

$$C_s = (A/\alpha) t^{-\alpha} (1 + Dt^\alpha) + B \quad (1)$$

where the coefficients may assume different val-

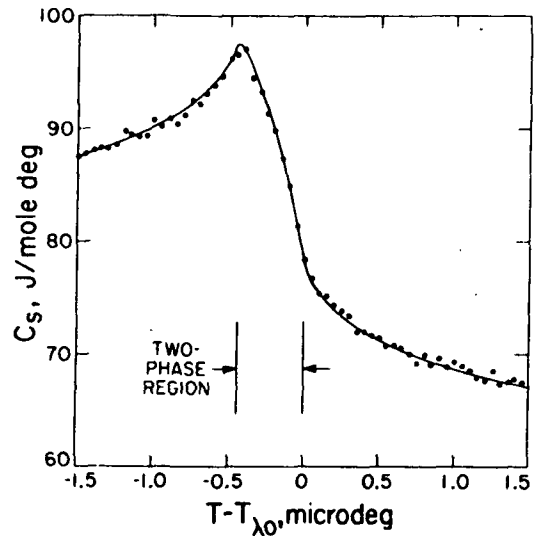


FIG. 2. Comparison of heat-capacity measurements with the predicted behavior (solid line) in the vicinity of the two-phase region.

ues on each side of the transition. The effect of gravity was calculated in three different ways, all based on the assumption³ that the heat capacity $C(T, h)$ of a given element of the sample at depth h below the surface is given by (1) but with t replaced by $t_h = |1 - T/T_{\lambda h}|$. Here $T_{\lambda h}$ is the local value of the transition temperature given by $T_{\lambda h} = T_{\lambda 0} + \rho g h / S_\lambda$ where ρ is the density of the liquid, g is the acceleration due to gravity, and S_λ is the slope of the λ line. Initially, the heat capacity of the sample was calculated simply by integrating $C(T, h)$ over the height H of the sample. This function was then fitted to the raw data outside the two-phase region by a standard least-squares procedure. Using a second approach, we first calculated $C(T, 0)$, the heat capacity at the gas-liquid interface, from the observations and then fitted (1) to the corrected data. Unfortunately, because of the negative slope of the λ line, both these methods yield no information in the temperature interval δT_2 below $T_{\lambda 0}$, which degrades the accuracy of the determination of α' . To improve this situation we modified the second method below T_λ to calculate the heat capacity at the *bottom* of the sample, and then incremented the temperature of each datum point by an amount δT_2 . This approach makes use of the relationship $C(T, H) = C(T + \delta T_2, 0)$ which is a direct consequence of the assumption described above, and generates estimates of $C(T, 0)$ with the desired distribution about $T_{\lambda 0}$. The three methods used to correct for the gravity distortion were found

to give similar results for the optimum parameter values: Here we describe the results obtained with the last method, for which the uncertainties were least.

In the curve-fitting analysis we rejected the data in the two-phase region because of larger uncertainties in the gravity corrections arising from the rapid variation of the correlation length with height near the phase boundary.¹⁰ Outside this region, we estimate such contributions to be less than ± 0.03 J/mole K, which is negligible for our purposes. Initially, gravity corrections corresponding to a logarithmic singularity in C_s were calculated; they were then updated with use of the first estimate of the best-fit parameters to our data. Finally, the best-fit parameters were redetermined, and found to be consistent with the previous set. From this information we calculated the heat capacity of the sample through the two-phase region and compared it with the observations. This curve is shown in Fig. 2. It can be seen that we obtain a very good fit even when the uncertainties in the estimated gravity effect are relatively large. This reinforces our belief that we have observed the equilibrium heat capacity of the sample throughout this region. To our knowledge this is the first time such data have been reported. We then used the data within and near the two-phase region to decrease the uncertainties in the estimate of $T_{\lambda 0}$, which was previously a free parameter. This point was determined to within ± 10 nK by comparing the data with the calculated functional form, and was then used as a constraint in the remainder of the curve-fitting analysis. In Fig. 3 we show the data, corrected for the effect of gravity, on a logarithmic temperature scale plotted relative to $T_{\lambda 0}$. The $C(T, 0)$ data below T_λ extend closer to $T_{\lambda 0}$ than the boundary of the two-phase region because of the temperature increment δT_2 which is part of the gravity correction.

A simultaneous estimate of all five free parameters in (1) on each side of T_λ leads to unacceptably large uncertainties in α , α' , and A/A' , the quantities of primary interest. Instead, we set D and D' equal to the values determined by Ahlers⁴ (-0.022 , -0.020), and $x = x' = 0.5$, close to the RG estimate, and evaluated the remaining parameters. This approach gave the results $\alpha = -0.0129 \pm 0.0033$, $\alpha' = -0.0125 \pm 0.0036$, and $B - B' = 0 \pm 4.4$, where the uncertainties correspond to the 2σ statistical confidence limit and the analysis covers the range $3 \times 10^{-8} \leq t \leq 10^{-3}$. It is clear that these results support the scaling pre-

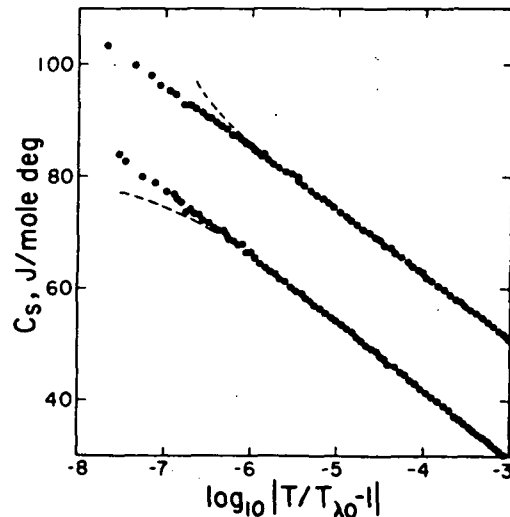


FIG. 3. Heat-capacity measurements over a wide range of temperature (upper curve, $T < T_\lambda$; lower curve, $T > T_\lambda$) corrected for the effect of gravity as described in the text. Below T_λ this correction includes a displacement of the data closer to the transition by an amount δT_2 . The broken lines show the location of the data before the gravity corrections were applied.

diction $\alpha = \alpha'$ and that the heat capacity is continuous through T_λ . With the additional constraint $\alpha = \alpha'$ we obtained $\alpha = -0.0127 \pm 0.0026$, $A/A' = 1.058 \pm 0.004$, and $B - B' = 0.1 \pm 3.1$. Since improved estimates for D and D' may become available, we determined the sensitivity of our results to changes in these parameters. For the optimum values of α and A/A' we obtained sensitivities $d\alpha/dD = -0.105 \pm 0.01$ and $d(A/A')/dD = (-2.7 \pm 0.3) \times 10^{-3}$ for a simultaneous change of the same magnitude in both D and D' . Thus a 50% change in the values of D and D' would not change our results significantly.

Our experiment can be compared with two classes of previous measurements made further from the λ point. Three sets of directly comparable heat-capacity measurements^{3,6} give¹¹ $-0.016 \leq \alpha \leq -0.020$ and $1.068 \leq A/A' \leq 1.081$ in the range $t \geq 10^{-6}$. With the additional assumption of universality our results can also be compared with experiments along the λ line⁵ and as a function of ^3He concentration,⁶ which give $-0.022 \leq \alpha \leq -0.026$ and $1.088 \leq A/A' \leq 1.11$ for $t \geq 5 \times 10^{-6}$. Our results, obtained from data extending significantly closer to the transition, give somewhat better agreement with the RG predictions¹ ($\alpha = -0.007 \pm 0.006$ and $A/A' \approx 1.03$) than those obtained previously. Further improvements in resolution will require either a more careful treatment of the

distortions near T_λ or a reduction in gravity, for example by performing the measurements in space.

We wish to thank W. M. Fairbank for his support and encouragement during this project. This work was supported by NASA Contracts No. JPL 955057 and No. NAG2-62, by National Science Foundation Grant No. DMR 8218989, and by the Research Corporation.

¹J. C. LeGuillou and J. Zinn-Justin, *Phys. Rev. B* **21**, 3976 (1980), and E. Brézin, J. C. Le Guillou, and J. Zinn-Justin, *Phys. Lett.* **47A**, 285 (1974).

²Preliminary results were reported by J. A. Lipa, *Physica (Utrecht)* **107B**, 343 (1981). More recent measurements [see *Proceedings of the Seventy-Fifth Jubilee Conference on ⁴He*, St. Andrews, Scotland, 1983 (to be published)] give very good agreement with

the data reported here. Major improvements to the apparatus were made since the preliminary work. A complete report is in preparation.

³G. Ahlers, *Phys. Rev. A* **3**, 696 (1971).

⁴See for example, G. Ahlers, in *The Physics of Liquid and Solid Helium*, edited by K. H. Bennemann and J. B. Ketterson (Wiley, New York, 1976), Pt. I.

⁵K. J. Mueller, G. Ahlers, and F. Pobell, *Phys. Rev. B* **14**, 2096 (1976).

⁶T. Takada and T. Watanabe, *J. Low Temp. Phys.* **41**, 221 (1980); F. M. Gasparini and M. R. Moldover, *Phys. Rev. B* **12**, 93 (1975).

⁷J. A. Lipa, B. C. Leslie, and T. C. Wallstrom, *Physica (Utrecht)* **107B**, 331 (1981).

⁸L. E. deLong, O. G. Symko, and J. C. Wheatley, *Rev. Sci. Instrum.* **42**, 147 (1971).

⁹G. Ahlers, *Phys. Rev. Lett.* **21**, 1159 (1968).

¹⁰M. R. Moldover, J. V. Sengers, R. W. Gammon, and R. J. Hocken, *Rev. Mod. Phys.* **51**, 79 (1979).

¹¹Some of these estimates are contained in F. M. Gasparini and A. A. Gaeta, *Phys. Rev. B* **17**, 1466 (1978).

HIGH RESOLUTION HEAT CAPACITY MEASUREMENTS NEAR THE LAMBDA-TRANSITION*

T. C. P. Chui and J. A. Lipa

Physics Department, Stanford University, Stanford, CA 94305

In the last few years the renormalization group (RG) technique has gained wide acceptance as the primary analytical tool for the studies of cooperative phase transitions. We have performed heat capacity measurements which extend to within 30 nano-deg of the lambda transition, subjecting the RG predictions to stringent experimental tests.

Figure 1 shows a cross section of the OHFC copper sample chamber, which incorporates an indium-sealed valve. After the annular helium space was 80% filled with liquid and the valve shut, the capillary was evacuated and then cryopumped throughout the experiment. Two such sample chambers with depths of 3 mm and 0.3 mm were used in two separate runs.

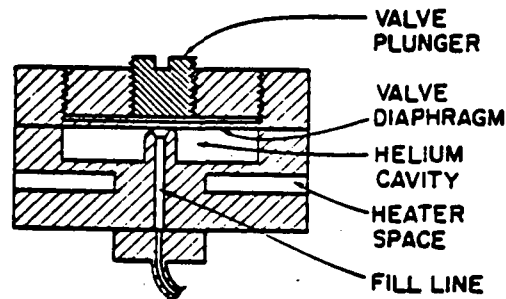


Fig. 1: Schematic view of sample chamber

Relative temperatures were measured using a paramagnetic salt thermometer¹ with a resolution of 6×10^{-10} deg in a 1 Hz bandwidth. The sample chamber was suspended from an isolation platform² by low thermal conductivity stainless steel supports. The temperature of the isolation platform was kept constant during measurements with another paramagnetic salt thermometer and an integrating servo loop. Two further stages of servo-controlled thermal isolation separated the sample from the main helium bath.

Sample 1 used the 3 mm deep cavity. This sample depth was chosen so that by far the largest distortion near the transition was the easily calculable gravitational effect.³ 50 nano-deg. from the transition the correlation length is about 0.04 mm, 1.5% of the sample height.⁴ Though the correction to the heat capacity due to finite correlation length is not well known, it reasonably can be expected to be less than 1.5%. Our data is

Table 1: Measured parameters compared to the RG predictions, using standard notation^{2,4}.

Parameter	Present Experiment	RG Prediction ^{6,7}
$\alpha(=\alpha')$	$-0.0138 \pm .0025$	$-.0079 \pm .003$
A/A'	$1.057 \pm .004$	1.03
$B-B'$	0.1 ± 3	0

shown in Figure 2 together with the fitted curve based on the simple gravitational correction.³ The two-phase region is well resolved. In Table 1 our best fit parameters are compared with the RG predictions.^{6,7}

Sample 2 was .3 mm deep. At $T - T_\lambda = 50$ nano-deg the correlation length now amounts to 1.5% of the sample height, yet our preliminary data still follows the curve based only on the gravitational effect, to within the accuracy of the data. This confirms that the correction due to the finite correlation length is indeed small.

Recently we have completed some measurements on a 0.03 mm sample using the .3 mm deep cavity. In this sample the transition should be significantly distorted by the size effect.⁵ Unfortunately, the signal-to-noise ratio is not yet good enough to resolve below about 200 nano-deg with this sample, too coarse to observe such an effect. Further improvements in thermometry may soon bring such an experiment within the realm of possibility.

We conclude that finite size corrections in a 3 mm sample are small. When allowance is made for the effect of gravity, our data fit the RG predictions better than previous experiments.

* This work supported by NASA Contracts # NAG2-62 and # 955057.

1. J. A. Lipa, B. C. Leslie and T. C. Wallstrom, *Physica* **107B**, 331 (1981).
2. J. A. Lipa and T. C. P. Chui, submitted to *Phys. Rev. Lett.*
3. G. Ahlers, *Phys. Rev. A* **3**, 696 (1971).
4. G. Ahlers, *Quantum Liquids*, eds: J. Ruvalds & T. Regge (North Holland, 1978).
5. G. Ahlers, *Phys. Rev.* **171**, 275 (1968).
6. J. C. Le Guillou and J. Zinn-Justin, *Phys. Rev. Lett.* **39**, 95 (1977).
7. E. Brezin, J. C. Le Guillou and J. Zinn-Justin, *Phys. Lett.* **47A**, 285 (1974).

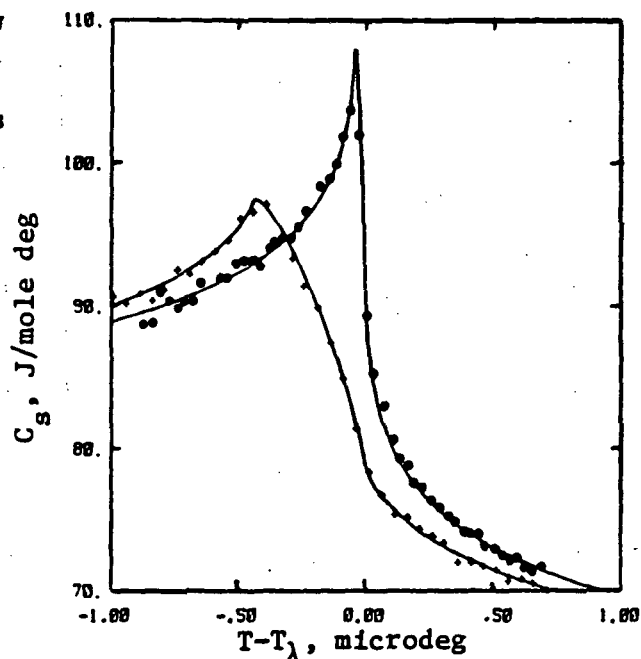


Fig. 2: Comparison of heat capacity measurements with predicted behavior (solid line) in the vicinity of the two phase region. +: 3 mm sample, •: 0.3 mm sample